



ALMA MATER STUDIORUM
UNIVERSITÀ DI BOLOGNA

ARCHIVIO ISTITUZIONALE
DELLA RICERCA

Alma Mater Studiorum Università di Bologna Archivio istituzionale della ricerca

Influence of sizing strategy and control rules on the energy saving potential of heat pump hybrid systems in a residential building

This is the final peer-reviewed author's accepted manuscript (postprint) of the following publication:

Published Version:

Dongellini Matteo, Naldi Claudia, Morini Gian Luca (2021). Influence of sizing strategy and control rules on the energy saving potential of heat pump hybrid systems in a residential building. ENERGY CONVERSION AND MANAGEMENT, 235, 1-12 [10.1016/j.enconman.2021.114022].

Availability:

This version is available at: <https://hdl.handle.net/11585/843167> since: 2024-05-13

Published:

DOI: <http://doi.org/10.1016/j.enconman.2021.114022>

Terms of use:

Some rights reserved. The terms and conditions for the reuse of this version of the manuscript are specified in the publishing policy. For all terms of use and more information see the publisher's website.

This item was downloaded from IRIS Università di Bologna (<https://cris.unibo.it/>).
When citing, please refer to the published version.

(Article begins on next page)

This is the final peer-reviewed accepted manuscript of:

Matteo Dongellini, Claudia Naldi, Gian Luca Morini

Influence of sizing strategy and control rules on the energy saving potential of heat pump hybrid systems in a residential building

In: Energy Conversion and Management, Volume 235, 2021, 114022

The final published version is available online at:

<https://doi.org/10.1016/j.enconman.2021.114022>

Terms of use:

Some rights reserved. The terms and conditions for the reuse of this version of the manuscript are specified in the publishing policy. For all terms of use and more information see the publisher's website.

This item was downloaded from IRIS Università di Bologna (<https://cris.unibo.it/>)

When citing, please refer to the published version.

1
2
3
4
5
6
7
8
9
10
11
12
13
14
15
16
17
18
19
20

Influence of sizing strategy and control rules on the energy saving potential of heat pump hybrid systems in a residential building

Matteo Dongellini^{a,*}, Claudia Naldi^a, Gian Luca Morini^a

^a Department of Industrial Engineering

Alma Mater Studiorum - University of Bologna

Viale Risorgimento 2, 40136, Bologna, Italy

*Corresponding author:

Tel: +39 051 2090567

Fax: +39 051 2093296

E-mail: matteo.dongellini@unibo.it

Other e-mails: claudia.naldi2@unibo.it; gianluca.morini3@unibo.it

21 **ABSTRACT**

22 Hybrid heat pump systems are a suitable solution to mitigate the well-known
23 disadvantages of air-source heat pumps, such as energy losses linked to defrost cycles
24 and a significant reduction of their heating capacity during the most severe part of the
25 season: in hybrid systems the heat pump is sized to satisfy only a fraction of the building
26 peak load and is coupled to a second heater (back-up device), which helps the heat pump
27 during the coldest part of the winter. In this paper, a series of dynamic simulations has
28 been performed to calculate the seasonal performance of hybrid systems based on an air-
29 to-water heat pump and to assess the optimal configuration of the system. Results point
30 out that the energy performance of these systems strongly depends on the heat pump
31 sizing, the back-up device typology and the control algorithm used for the activation of
32 the heat generators. It is demonstrated that the adoption of hybrid systems in which the
33 heat pump is coupled to a gas boiler allows to obtain relevant primary energy savings.
34 The overall seasonal efficiency can be increased up to 6% and 22%, if compared to
35 monovalent systems respectively based on a heat pump or a gas boiler, only if the heaters
36 are activated following an alternative operating mode, with a cut-off temperature selected
37 between the design and the bivalent temperature. On the contrary, if the back-up device
38 of the hybrid system is an electric resistance, the heaters have to work in parallel during
39 the whole heating season and the only achievable advantage is that the heat pump can be
40 slightly under-sized with respect to the nominal building load.

41

42 **Keywords:** hybrid heat pump system; air-to-water heat pump; gas-fired boiler; cycling
43 losses; control strategy; system energy performance.

44

45 **NOMENCLATURE**

46 *Abbreviations*

| | | |
|----|------|------------------------------|
| 47 | AWHP | Air-to-water heat pump |
| 48 | B | Boiler |
| 49 | BES | Building energy signature |
| 50 | EEV | Electronic expansion valve |
| 51 | ER | Electric resistance |
| 52 | HDD | Heating degree day |
| 53 | HHP | Hybrid heat pump |
| 54 | HP | Heat pump |
| 55 | LHV | Lower heating value |
| 56 | TEV | Thermostatic expansion valve |
| 57 | TMY | Typical meteorological year |

58

59 *Symbols*

| | | | |
|----|----------------------------|----------------------------|-------------------------|
| 60 | <i>COP</i> | Coefficient of performance | |
| 61 | <i>E</i> | Energy | (kWh) |
| 62 | <i>K_p</i> | Proportional gain | |
| 63 | <i>P</i> | Power | (kW) |
| 64 | <i>PEF</i> | Primary energy factor | (kWh _p /kWh) |
| 65 | <i>t</i> | Time | (s) |
| 66 | <i>T</i> | Temperature | (°C) |
| 67 | <i>T_{biv}</i> | Bivalent temperature | (°C) |
| 68 | <i>T_{cut-off}</i> | Cut-off temperature | (°C) |

| | | | |
|----|----------------------|---|------|
| 69 | T_{des} | Design temperature | (°C) |
| 70 | t_i | Integral time | (s) |
| 71 | $SCOP$ | Seasonal coefficient of performance | |
| 72 | $SCOP_{net}$ | Net seasonal coefficient of performance | |
| 73 | | | |
| 74 | <i>Greek symbols</i> | | |
| 75 | β | Peak load ratio | |
| 76 | η_B | Boiler seasonal efficiency | |
| 77 | η_{ER} | Electric resistance seasonal efficiency | |
| 78 | η_g | Boiler efficiency | |
| 79 | η_s | Heating system seasonal efficiency | |
| 80 | τ | Time constant | (s) |
| 81 | φ | Part load factor | |
| 82 | Φ | Inverter frequency | (Hz) |
| 83 | | | |
| 84 | <i>Subscripts</i> | | |
| 85 | bu | back-up heater | |
| 86 | del | delay | |
| 87 | des | design | |
| 88 | ee | electric energy | |
| 89 | ext | external | |
| 90 | gas | natural gas | |
| 91 | gen | main heat generator | |
| 92 | h | heating | |

| | | |
|-----|------------|------------------------------|
| 93 | <i>j</i> | index for j-th heater |
| 94 | <i>i</i> | index for i-th energy vector |
| 95 | <i>in</i> | inlet |
| 96 | <i>off</i> | shut-down transient |
| 97 | <i>on</i> | start-up transient |
| 98 | <i>out</i> | outlet |
| 99 | <i>p</i> | primary |
| 100 | <i>set</i> | set-point |
| 101 | <i>th</i> | thermal |
| 102 | <i>tot</i> | total |
| 103 | <i>w</i> | water |

104

105 **1. INTRODUCTION**

106 Nowadays it is well established that the building sector significantly contributes to
 107 primary energy demand and greenhouse gas (GHG) emissions of the developed countries
 108 [1]. The European Commission agreed on a series of challenging targets to be achieved
 109 before 2030 [2]-[5]: (i) 40% reduction of GHG emissions with respect to 1990 levels; (ii)
 110 at least 27% share of renewable energy sources (increased to 32% in 2018) and (iii) at
 111 least 27% energy efficiency increase with respect to the baseline scenario (upgraded to
 112 32.5% in 2018).

113 Due to the dramatic crisis of the construction sector which occurred during the last years,
 114 it is common knowledge that the above-mentioned targets can only be achieved by
 115 renewing the existing building stock: for example, in Italy the annual rate of new
 116 constructions is very low and ranges within 0.1-0.2% of the actual building stock [6]. The

117 primary energy consumption of existing buildings can be reduced with the refurbishment
118 of the building envelope components and/or with the retrofit of the Heating, Ventilation
119 and Air Conditioning (HVAC) system.

120 In this frame, electric heat pumps may represent a promising solution to achieve the
121 environmental targets introduced by the European Union. In fact, under current electricity
122 grid mixes, in the major part of the world regions this kind of devices are already less
123 GHG emission intensive than traditional HVAC systems based on fossil fuels [7]-[8]. In
124 addition, heat pumps have the potential to exploit a significant amount of renewable
125 energy by using aerothermal, geothermal and hydrothermal energy sources during their
126 operation [9]. Moreover, in recent years the use of heat pumps in HVAC systems has
127 spread widely for many other reasons [10]: (i) the capability to cover with a single device
128 both space heating and cooling, as well as domestic hot water production; (ii) the strong
129 improvement of their energy performance and reliability; (iii) the wider diffusion of on-
130 site renewable electric energy generators as PV systems and the evolution of electricity
131 prices [11].

132 In the European market, outdoor air is the most widespread heat source for heat pumps
133 [10]. Air-source devices have a lot of well-known benefits, such as the availability of the
134 external source and their low investment cost (with respect to ground-source and water-
135 source units); on the other hand, their diffusion is held back by several unfavorable
136 characteristics which do not allow to completely exploit the energy saving potential of
137 these devices. First, during the coldest part of the heating season, the air-source heat pump
138 heating capacity is reduced and its Coefficient of Performance (*COP*) decreases, while
139 the building thermal load is at its maximum value [12]. Moreover, the well-known
140 phenomenon of the frost deposition on the outdoor heat exchanger surface during the

141 most severe period of the heating season and the consequent energy losses linked to
142 defrosting cycles penalize the seasonal energy performance of these devices. More in
143 detail, the degradation effect of frosting phenomena is twofold: on the one hand,
144 defrosting cycles lower the heat pump heating capacity and the overall energy efficiency
145 of the system [13]; on the other hand, the unavoidable interruption of indoor heating
146 during the cycles may adversely affect the building occupants' thermal comfort [14].

147 Last but not least, if the air-source heat pump is sized to cover the building peak load in
148 correspondence of the outdoor design temperature, the unit would operate at partial load
149 during the whole heating period, since the peak load occurs only for a limited period of
150 the season; for this reason, the seasonal performance factor of the system could be
151 strongly reduced due to the excessive number of on-off cycles, activated even in presence
152 of inverter-driven compressors [15].

153 In order to mitigate and in some cases to avoid the highlighted drawbacks, one possible
154 solution is the adoption of hybrid heat pump (HHP) systems: in this configuration the air-
155 source heat pump is sized to cover only a fraction of the building peak load and a second
156 heat generator (also called back-up heater) supports the heat pump operation when its
157 heating capacity is insufficient. Moreover, the back-up device can also be operated in
158 place of the heat pump whenever its operation is not ecologically or economically viable.

159 The adoption of HHP systems can be crucial for the energy retrofit of heating systems in
160 existing buildings where high-temperature terminal units, such as cast-iron radiators, are
161 present. In fact, heat pumps are generally characterized by a limited temperature range
162 for the produced hot water, which can be only partially in agreement with the requests of
163 high-temperature terminal units. In this case, during the most severe period of the heating
164 season, when the required supply temperature increases, the back-up device can help the

165 heat pump to reach the desired supply temperature. Furthermore, the back-up heater can
166 reduce the negative effects due to defrosting by replacing the heat pump during the
167 activation of defrost cycles. Last but not least, in existing buildings where a conventional
168 generation system based on a gas/oil boiler is present, the boiler can be fruitfully used as
169 back-up device with no additional investment costs.

170 At the moment, the market share of hybrid heat pump systems in Europe is still limited
171 but is rapidly growing. In 2014 only about 6500 HHP systems were sold in the whole
172 European market but in 2017 almost 6700 HHP devices were sold by considering only
173 the Italian market, doubling the sales of HHP in Italy of 2015 [16]. Moreover, a recent
174 study on the European market of HHPs shows that a number of sales close to 40000 HHPs
175 units is expected in 2020 [17].

176 Due to the increasing interest of the market for HHP systems, a series of scientific works
177 has been recently conducted with the aim to investigate and optimize the energy
178 performance of different kinds of hybrid systems involving air-source heat pumps and
179 back-up heaters.

180 Park et al. [18] developed a numerical model of a hybrid system consisting of an air-to-
181 water heat pump (AWHP) and a gas-fired water heater coupled to a typical residential
182 apartment. The energy performance and the economic feasibility of the proposed system
183 were investigated by the authors, who concluded that the achievable energy savings are
184 strongly influenced by the effective control strategy of the hybrid water heater. The
185 importance of control algorithms for these systems has been also highlighted by De
186 Coninck and Helsen [19]: they implemented a Modelica grey-box model of a HHP system
187 composed by two AWHPs and a condensing gas boiler, comparing the efficiency of a
188 model-predictive and a rule-based control logic. Results pointed out that the predictive

189 controller could guarantee similar thermal comfort and energy cost savings up to 40%
190 with respect to the standard control. Li [20] proposed an innovative economic-based
191 control logic for a parallel loop hybrid system composed by an AWHP and a gas-fired
192 water heater. According to this logic, the optimal working point of the system (i.e. mass
193 flow rate and supply water set-point temperature for each device) can be evaluated and
194 significant economic benefits up to 60% can be obtained with respect to a traditional
195 solution. Li and Du [21] investigated the energy and economic performance of a hybrid
196 system in which an AWHP and a gas boiler are connected in series. They compared the
197 effectiveness of two control algorithms used for the activation of the heat generators and
198 the optimization of their operating modes. Results pointed out that with both control
199 strategies significant energy savings can be achieved and the best performance is obtained
200 when both heat devices are simultaneously activated. Furthermore, other researchers have
201 recently demonstrated that this topic is worth to be investigated: these analyses point out
202 that the optimization of HHP systems control logic by means of cost-adaptive and
203 demand-response algorithms is a simple and cost-effective solution to obtain with HHP
204 systems energy and economic savings up to 22% ([22]-[26]).

205 Another important parameter for the optimization of the energy savings achievable with
206 the adoption of HHP systems is the choice of the size of the heating system components
207 (boiler, heat pump, thermal storage) and its consequences on the algorithm by means of
208 which the control system decides to switch on or off the heaters. In the literature, few
209 studies have already focused on this topic. For instance, Bagarella et al. [27] analyzed, by
210 means of dynamic simulations, how the control system of the heaters of a hybrid system
211 (i.e. heat pump and gas boiler) affects the seasonal efficiency of the system. They
212 analyzed two different working modes for the hybrid system: i) the operating mode in

213 which heat pump and boiler are switched on alternatively; ii) the operating mode in which
214 heat pump and boiler work in parallel. The authors used the numerical results in order to
215 assess the optimal values of control setting for HHP systems. The same topic was studied
216 by Fischer et al. [28]: the optimal size of the main elements of a hybrid system (PV panels,
217 air-source heat pump, electric boiler and thermal storage) was investigated taking into
218 account electricity price, profile of space heating loads, domestic hot water demand and
219 photovoltaic field size. Results showed that, in order to obtain the maximum energy
220 performance, the profile of the heating load should be considered in detail. Similar results
221 have been obtained by Klein et al. [29]: annual simulations of a hybrid heat pump system
222 were performed by varying the insulation of the building envelope, the volume of the
223 thermal storage and the heat pump size; the results of this work highlight that the influence
224 of the thermal storage volume on the seasonal performance of the system is negligible
225 while the maximum efficiency can be achieved with heat pumps sized to cover only a
226 fraction of the building peak load. Furthermore, Di Perna et al. [30] compared the energy
227 performance of monovalent and bivalent heating systems considering different kinds of
228 heat generators (i.e. oil and gas boiler, micro CHP, heat pump) and back-up unit (i.e.
229 electric heater and gas boiler). They found that the electrical back-up systems are not a
230 profitable solution.

231 The analysis of the literature points out that only few studies on HHP systems include, at
232 the same time, a detailed modeling of both building and heating system components (i.e.
233 by taking into account the energy penalties due to defrosting and on-off cycles of the heat
234 pump), the evaluation of the best system layout and the optimization of the control
235 strategy. In this work a numerical investigation of the seasonal energy performance of a
236 HHP system composed by an air-to-water heat pump coupled in series to a back-up device

237 (an electric resistance or a condensing gas boiler) is presented. The analysis is focused on
238 the optimization of the HHP system energy performance during the winter season only,
239 that is often an important part of the annual operating time of heat pumps coupled to
240 residential buildings in cold climates. The dynamic model of the hybrid system has been
241 developed by means of TRNSYS 17 [31]. The main goal of this investigation is to analyze
242 the role played by the back-up typology (electrical resistance or gas-fired boiler), by the
243 system control logic and by the heat pump sizing with respect to the design building
244 heating load on the seasonal performance factor of the HHP system. A series of
245 simulations has been carried out, taking into account different configurations of the
246 system. In these simulations, unlike in the most part of similar works appeared recently
247 in the literature ([18]-[26], [28]), the energy losses linked to both the heat pump on-off
248 cycling and to the defrost cycles have been considered. These energy losses can strongly
249 influence the overall performance of a hybrid system based on an air-source heat pump
250 during the winter season (especially in climatic regions where the ambient temperature
251 stays between 0°C and 6°C during the winter, like in large part of Italy) and their
252 evaluation is crucial in order to obtain a realistic evaluation of the seasonal energy
253 performance of HHP systems [32].

254

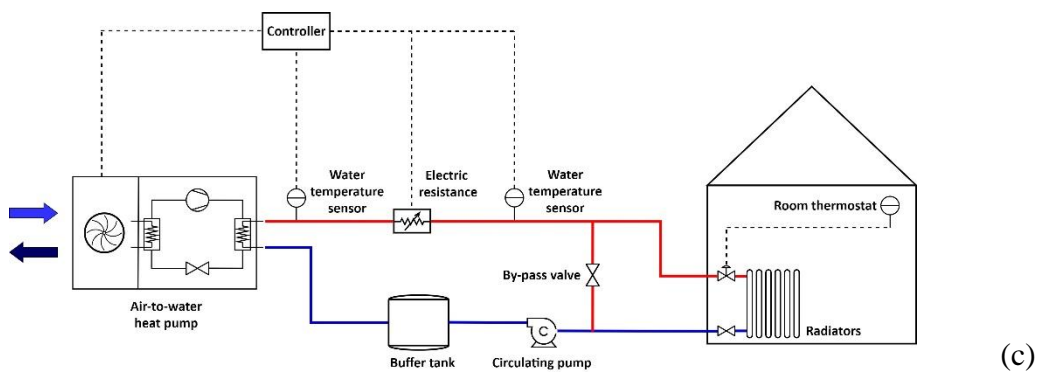
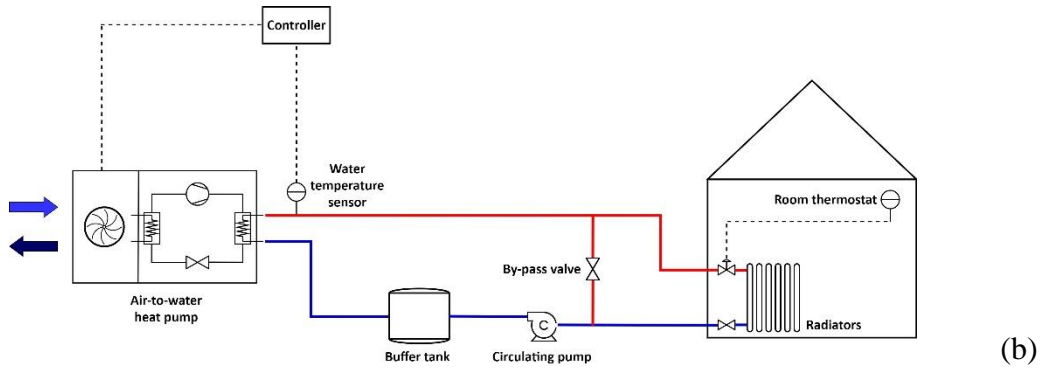
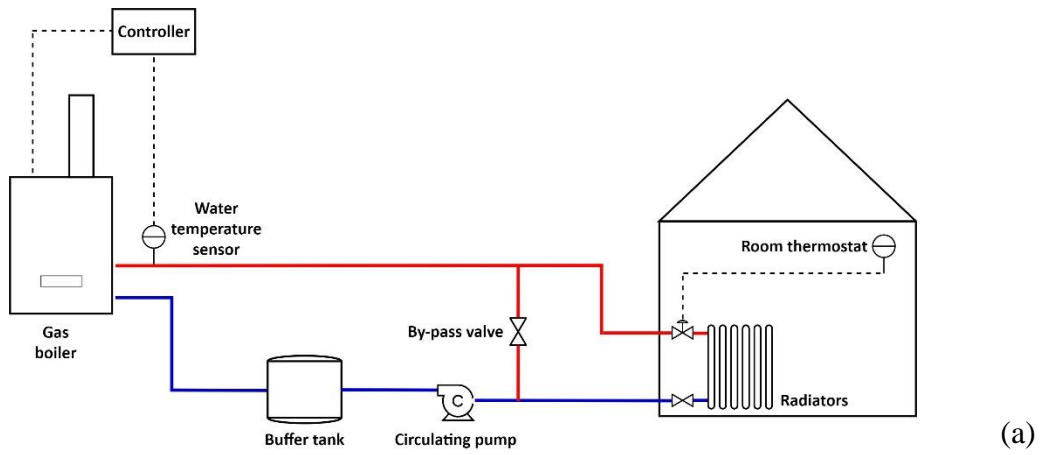
255 **2. METHODOLOGY**

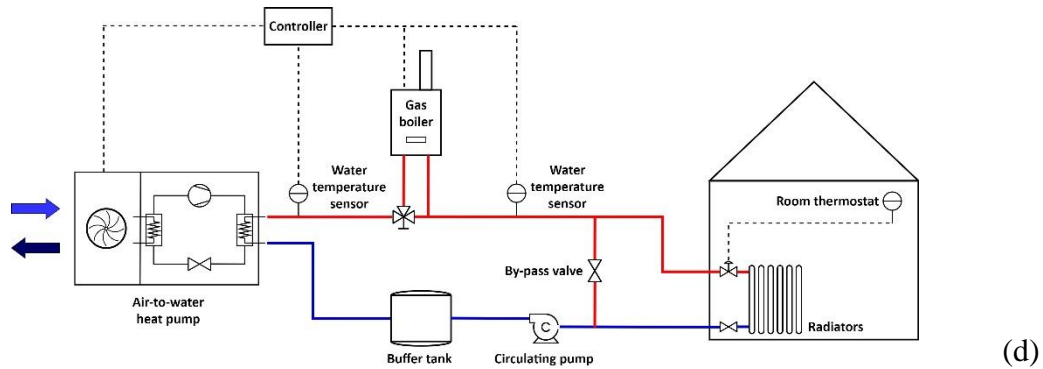
256 **2.1. Layout of simulated systems**

257 Different kinds of HHP systems and conventional heating systems based on a single
258 generator (condensing gas boiler or air-to-water heat pump) were firstly implemented in
259 TRNSYS in order to evaluate and compare their seasonal energy performance: in Figure
260 1 the layout of the simulated systems is shown. ~~It is important to stress that all the~~

261 elements reported in Figure 1 have been modelled within TRNSYS, by means of
262 components included in the standard libraries of the software and by means of innovative
263 dynamic models developed by the Authors and described in [33].

264





265 *Figure 1. Layout of the simulated heating systems: (a) condensing gas boiler only, (b) air-to-water heat*
 266 *pump only, (c) HHP system based on air-to-water heat pump and electric resistance, (d) HHP system*
 267 *based on air-to-water heat pump and condensing gas boiler.*
 268

269 All the elements reported in Figure 1 have been modelled in TRNSYS, by using standard
 270 components included in the software libraries as well as original dynamic models
 271 developed by the Authors and described in [33]. More in detail, the basic elements of the
 272 heating systems have been modelled with standard components: Type534 is used for the
 273 buffer tank, Type114 simulates the single speed pump, while the radiators consist of a
 274 series of Types 362. The system control logics have been implemented through Type2d
 275 (on-off thermostat) and Type23 (PID controller). The performance of the condensing gas
 276 boiler has been evaluated with the boiler block (Type700) in combination with Type581;
 277 by means of which the efficiency of this device has been calculated. Electric resistances
 278 were simulated with Type6 (auxiliary heater), while specific components, as introduced
 279 by the Authors in Ref. [33], has been used to simulate the behavior of the inverter-driven
 280 air-to-water heat pumps.

281 First of all, the monovalent systems illustrated in Figure 1a and Figure 1b are considered
 282 as baselines for the energy performance analysis carried out in this paper. In these
 283 configurations the heating system is based on a single heat generator, a gas boiler (Figure
 284 1a) or an air-to-water heat pump (Figure 1b). In these cases, the generator has been sized

285 to cover the building heating peak load; in this way, the required energy demand of the
286 building is matched during the whole winter season.

287 On the contrary, in HHP systems the air-to-water heat pump is coupled to a back-up
288 device (electrical heater in Figure 1c or gas boiler in Figure 1d, respectively). In these
289 cases, the heat pump size is reduced because a fraction of the heating load is covered by
290 the back-up system. The heat generators of these configurations are connected in series,
291 in order to improve the heat pump energy performance according to a lower sink
292 temperature.

293 As can be seen in Figure 1, a small water buffer tank is present in the hydronic loop for
294 each configuration in order to increase the thermal inertia of the system. The buffer tank
295 is a commercial 79 liters water storage having a well-insulated blanket (U-value equal to
296 $0.8 \text{ W/m}^2\text{K}$). The considered thermal storage allows to limit the frequency of the heat
297 pump on-off cycles under 6 start-ups per hour, which is the maximum value
298 recommended by the heat pump manufacturer.

299 Each thermal zone is heated by a single terminal unit, sized on the design load of the
300 room. The emitters are low-temperature radiators, each one equipped with a thermostatic
301 valve. The design supply temperature $T_{w,des}$ (i.e. the supply water temperature in
302 correspondence of the design outdoor temperature T_{des}) has been set equal to 55°C and
303 the design water flowrate has been calculated for each radiator by fixing a nominal
304 temperature difference of 10 K. Moreover, the set-point temperature of the supply hot
305 water to the emitters ($T_{w,set}$) is variable during the heating season and depends on the
306 outdoor air temperature: in each configuration the heat generator produces hot water at
307 the same temperature as the value given by the climatic curve reported in [34].

308 A by-pass valve guarantees the effectiveness of the variable flow rate emitters and ensures
 309 the correct operation of the constant-speed circulating pump. In fact, the hot side water
 310 flow is split between the emitters and the by-pass loop according to the thermostatic valve
 311 opening,

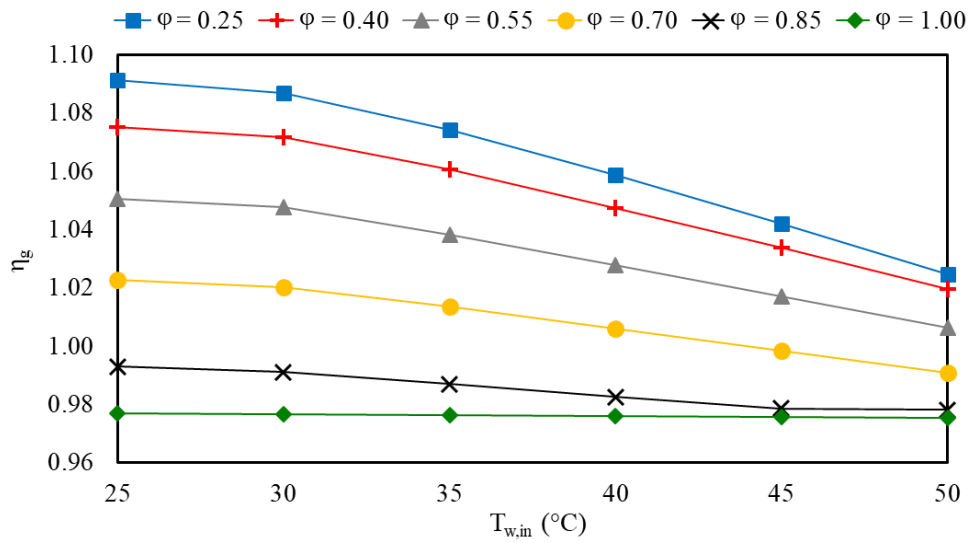
312 The boiler used in these simulations is a condensing gas-fired unit. The dynamic model
 313 of this device is based on a performance-map approach: the performance data of a
 314 commercial boiler, as reported by the technical datasheets of the manufacturer, have been
 315 used to build the look-up table introduced in the model. The main technical characteristics
 316 of the selected unit are reported in Table 1 and the boiler efficiency referred to the Lower
 317 Heating Value (LHV), η_g , is shown in Figure 2 as a function of the part load factor, φ ,
 318 and of the return water temperature, $T_{w,in}$. Reported data highlight that the boiler is
 319 characterized by an efficiency larger than 1 only for load factors lower than 0.70.

320

321 Table 1. Condensing boiler technical data.

| Parameter | Value |
|--|-------------|
| Nominal heating capacity (supply/return water temperature = 80/60°C) | 21.5 kW |
| Nominal η_g (supply/return water temperature = 80/60°C) | 97.5% |
| Heating capacity modulation range | [0.25-1.00] |
| $\tau_{on,h,B}$ | 125 s |
| $\tau_{off,h,B}$ | 0 s |

322



323

324

325

Figure 2. Boiler efficiency as a function of return water temperature and part load factor.

326

327

328

329

330

331

332

333

334

335

336

337

The energy losses linked to the boiler on-off cycles have been taken into account: although the unit is characterized by a broad modulation range ([0.25-1.00], see Table 1), when the building heating load is very low, on-off cycles must be performed by the boiler and its efficiency decreases due to the heat losses from the generator casing and the exhaust gases [30]. Following the methodology described by Dongellini and Morini [33], the boiler start-up losses have been considered by introducing an exponential corrective factor for the boiler heating capacity during the start-up transient. The time constant of this phase ($\tau_{on,h,B}$) has been evaluated experimentally by the boiler manufacturer and its value is reported in Table 1. Similarly, the boiler behavior during the shut-down transient has been evaluated but, in this case, the delivered heating power becomes zero when the device is switched off and no recovery effects are considered. For this reason, the time constant of the shut-down transient ($\tau_{off,h,B}$) is set equal to zero.

338

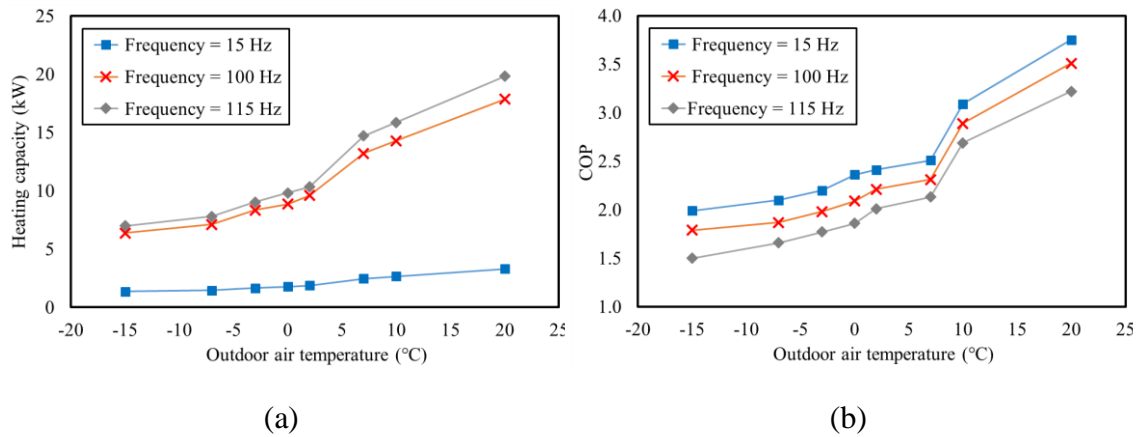
339

340

341 Table 2. Technical data of the selected air-to-water inverter-driven heat pump

| Parameter | Value |
|--|--|
| Nominal heating capacity ($T_{ext} = 7^{\circ}\text{C}$, supply/return water temperature = $55/45^{\circ}\text{C}$) | 14.7 kW |
| Nominal COP ($T_{ext} = 7^{\circ}\text{C}$, supply/return water temperature = $55/45^{\circ}\text{C}$) | 2.13 |
| Refrigerant | R410A |
| Compressor data | Twin rotary variable speed device (frequency range: 15-115 Hz) |
| $\tau_{on,h,HP}$ | 35 s |
| $\tau_{off,h,HP}$ | 0 s |
| $\tau_{on,ee,h,HP}$ | 10 s |
| $\tau_{off,ee,h,HP}$ | 0 s |

342



343
344
345

Figure 3. Full load and partial load heat pump performance data for water supply/return temperature equal to $55/45^{\circ}\text{C}$: heating capacity (a) and COP (b) as functions of the outdoor air temperature.

346 The AWHP unit considered in the simulations is an inverter-driven heat pump based on
347 a compression cycle. The unit has been modelled by using a performance-map approach,
348 as described in [33]. The heat pump heating capacity and COP are evaluated by means of
349 a three-dimensional look-up table as a function of the inverter frequency, Φ , and of the
350 sink and source temperatures (i.e. return water temperature, $T_{w,in}$ and external air
351 temperature, T_{ext} , respectively). These data have been obtained by a series of experimental
352 measures made in collaboration with the heat pump manufacturer. In Table 2 and Figure
353 3 the main technical data, and the full load and partial load performance data of the
354 modelled heat pump are reported, respectively.

355 Since the AWHP is sized on the building design load, the unit modulates its delivered
356 thermal capacity during the milder part of the season to meet the building energy demand.
357 For this reason, the heat pump carries out a significant number of on-off cycles when a
358 further modulation of the compressor speed is not possible (i.e. in correspondence of the
359 hottest part of the heating season). The energy losses linked to the heat pump on-off
360 cycling have been taken into account by using the model described in [33]: the energy
361 performance of the unit is reduced at each start-up because the pressure difference
362 between high- and low-pressure sides must be restored. This degradation effect consists
363 on a reduction of the unit heating capacity, rather than on an increase of the electrical
364 power input [35]: experimental tests conducted in collaboration with the heat pump
365 manufacturer allowed to measure the duration of the start-up transient and to evaluate the
366 characteristic time constants of the heat pump ($\tau_{on,h,HP}$, $\tau_{off,h,HP}$, $\tau_{on,ee,h,HP}$, $\tau_{off,ee,h,HP}$), whose
367 values are reported in Table 2. It is important to highlight that the unit considered in this
368 work is equipped with an Electronic Expansion Valve (EEV), which guarantees lower

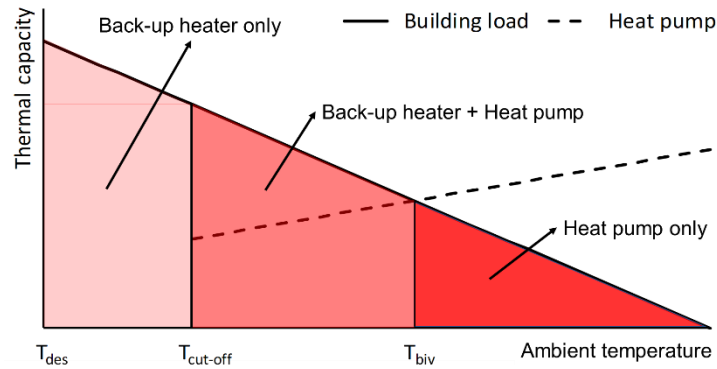
369 cycling losses with respect to a Thermostatic Expansion Valve (TEV), as highlighted in
370 [15].

371 Since the most widespread defrosting strategy for air-source heat pumps is the reverse
372 cycle method [36], a simplified model based on this technique, able to take into account
373 frost formation and defrosting energy losses, has been used in this work. Full details about
374 this simplified model can be found in Vocale et al. [37]. When a defrost cycle is
375 performed, the unit outdoor heat exchanger operates as a condenser and the indoor heat
376 exchanger acts as an evaporator. Before the cycle inversion, the heat pump is switched
377 off for about 1 minute: during this period the outdoor fans are stopped and the four-way
378 valve is reversed. After this stand-by period the unit operates in cooling mode and the
379 frost layer is melted. Finally, after another stand-by period (1 minute) the four-way valve
380 reverses again and the heat pump returns to the heating operating mode. The duration of
381 the defrost cycle typically ranges from 90 seconds to 8 minutes ([38]-[40]) and it is
382 defined by the heat pump controller. In this work each defrost cycle runs for 7 minutes (1
383 minute for the first stand-by period, 5 minutes for the cooling reversed mode and 1 minute
384 for the second stand-by period). Defrost cycles are performed by the heat pump regularly
385 at defined intervals: when the outdoor air temperature is below 5°C and at the same time
386 the relative humidity is above 75%, a defrost cycle is repeated each 45 minutes.

387 In the HHP configurations shown in Figure 1c and in Figure 1d, the heat pump and the
388 back-up heat generator are connected in series and can operate independently of one
389 another. The control system continuously monitors the temperature of the hot water
390 supplied by the heat pump and compares it with a set-point value: when the heat pump
391 heating capacity is lower than the building thermal load, the back-up device is switched

392 on. In the following Sections, further details on the system control algorithms will be
 393 given.

394



395

396 *Figure 4. Main parameters and possible operating modes of a hybrid heat pump system.*

397

398 In Figure 4 the operating modes and the main parameters related to HHP systems are
 399 presented. The bivalent temperature (T_{biv}) is shown in Figure 4 in correspondence of the
 400 point in which the building heating load (solid line) equals the heat pump heating capacity
 401 (dashed line).

402 Another parameter used for the analysis of this kind of systems is the peak load ratio, β .
 403 This parameter is defined in Eq. 1 as the ratio between the heat pump heating capacity at
 404 design conditions ($P_{HP}(T_{des})$), and the building peak load (P_{des}):

405

$$\beta = \frac{P_{HP}(T_{des})}{P_{des}} \quad (1)$$

406

407 For monovalent systems based on an AWHP only, the peak load ratio is equal to or larger
 408 than 1. In HHP systems, β ranges from 0 to 1: the higher the heat pump size, the higher
 409 the peak load ratio.

410 In addition, the cut-off temperature ($T_{cut-off}$) is here defined as the value of the ambient
411 temperature in correspondence of which the heat pump is switched off due to specific
412 control rules, typically related to energetic or economic considerations. When the outdoor
413 air temperature is below the cut-off temperature, the back-up device is the only active
414 heat generator.

415 If $T_{cut-off} = T_{biv}$, the hybrid system operates by switching on the back-up heater and
416 switching off the heat pump when $T_{ext} < T_{biv}$. In this case, the heating system works in
417 pure alternative mode. On the other hand, if the control system sets a cut-off temperature
418 lower than the bivalent temperature, both heat generators are switched on when $T_{cut-off} <$
419 $T_{ext} < T_{biv}$: in this case the heat generators operate in parallel. Furthermore, a pure parallel
420 configuration is set if $T_{cut-off}$ is fixed equal to the design temperature, T_{des} . In this case the
421 heat pump is active during the whole heating season, even for low values of the outdoor
422 temperature.

423

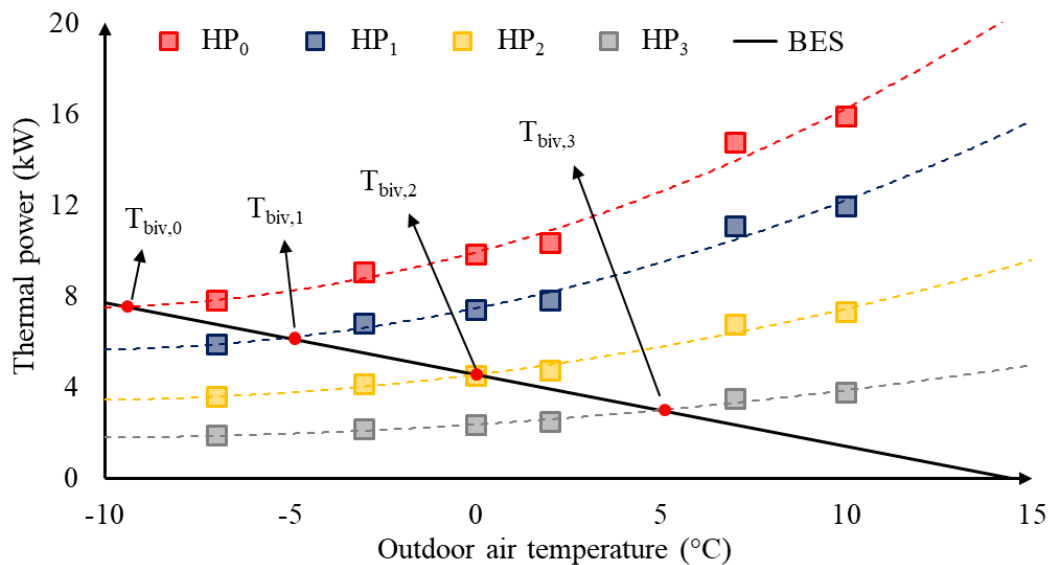
424 **2.2. Building modeling and climatic data**

425 The residential building SFH100 described by the report IEA SHC Task 44/HPP Annex
426 38 (T44A38) [34] has been considered as reference case study. The considered building
427 is characterized by a net heated volume of about 390 m³ and a heated floor area of 140
428 m². It represents a non-renovated existing house: the UA-value of the entire building is
429 290 W/K and its heating demand is equal to 100 kWh/(m² y) for the climate of Strasbourg.
430 Simulations have been performed for the Italian climate of Bolzano, a location placed in
431 the North of Italy and characterized by a cold and humid winter. According to current
432 Italian law [41], the heating system is switched on from October, 15th to April, 15th, for a

433 total of 183 days. The simulation timestep has been set equal to 30 s, in order to avoid
434 numerical and convergence issues.

435 The Typical Meteorological Year (TMY) of Bolzano reported within the TRNSYS
436 weather data library has been used to obtain the hourly climatic data: according to this
437 data, the design outdoor air temperature, T_{des} , is equal to -9°C , while the heating degree
438 days (HDDs) over the heating season, calculated with a base temperature of 20°C , are
439 2656. Furthermore, the heat generator operates 24/7 along this period and the internal set-
440 point temperature is set to 20°C along the whole season, with no night set-back.

441



442

443 *Figure 5. Performance data at full load of the considered heat pumps and building energy signature*
444 *(BES)*

445

446 The heat load of the building has been calculated by means of the TRNBUILD plugin of
447 TRNSYS [42]: in correspondence of the design ambient temperature (i.e. -9°C for
448 Bolzano) the design load of ground floor and first floor is equal to 3.11 and 4.27 kW,
449 respectively, corresponding to a peak load for the heat distribution system of 7.38 kW.
450 Moreover, according to the building energy signature method (BES) [43], the thermal

451 load required by the building during the heating season has been correlated to the external
 452 air temperature by means of a linear function: in Figure 5 the BES of the reference
 453 building is shown with a solid black line. It is evident that the required thermal load
 454 vanishes for outdoor temperatures higher than 15°C due to internal and solar heat gains.

455

456 2.3. Heating system configurations

457

458 Table 3. Performance data of the simulated heating systems (heat pump data evaluated
 459 for supply/return water temperatures equal to 55/45°C)

| Case | #1 | #2 | #3 | #4 | #5 | #6 | #7 | #8 |
|-----------------------------|-----------------|---------------------|---------------------|---------------------|--------------------|--------------------|--------------------|----|
| Heat generators | HP ₀ | HP ₁ +ER | HP ₂ +ER | HP ₃ +ER | HP ₁ +B | HP ₂ +B | HP ₃ +B | B |
| T_{biv} (°C) | -10 | -5 | 0 | +5 | -5 | 0 | +5 | / |
| P_{HP} (T_{des}) (kW) | 7.52 | 5.48 | 3.34 | 1.65 | 5.48 | 3.34 | 1.65 | / |
| P_{bu} (kW) | / | 1.90 | 4.04 | 5.73 | 21.5 | 21.5 | 21.5 | / |
| β | 1 | 0.74 | 0.45 | 0.22 | 0.74 | 0.45 | 0.22 | 0 |

460

461 In order to study the influence of the heat pump size on the seasonal energy performance
 462 of a HHP system, four air-to-water heat pumps (HP) have been considered in this work,
 463 coupled to electric resistances (ER) or to a gas-fired boiler (B). The main characteristics
 464 of the simulated units are summarized in Table 3.

465 In Figure 5 the heating capacity at full load of the heat pumps is reported as a function of
 466 the ambient temperature by fixing inlet/outlet water temperatures equal to 45/55°C,
 467 respectively. In that Figure, the heat pump used in the monovalent system has been
 468 referred to as HP₀, while the smaller units used in HHP systems have been indicated as

469 HP₁, HP₂ and HP₃, respectively. In addition, in Figure 5 and in Table 3 the bivalent
470 temperature of each configuration, T_{biv} , is also shown. It is evident that by scaling from
471 HP₀ to HP₃ the value of T_{biv} strongly increases and, for this reason, the peak load ratio, β ,
472 decreases. As a consequence, when undersized heat pumps are considered, the back-up
473 heater heating capacity, P_{bu} , increases in order to completely satisfy the building energy
474 demand. When an electric resistance is used as back-up unit in a HHP system, its rated
475 capacity is calculated as the difference between the building peak load and the heat pump
476 heat supply at design conditions. On the other hand, the condensing gas boiler considered
477 as back-up device in configurations #5-#7 is the same gas-fired unit described in Section
478 2.1 and used as single heat generator in the reference configuration shown in Figure 1a.
479 It is important to highlight that when the heat pump size decreases, passing from HP₀ to
480 HP₃, the peak load ratio decreases from 1 to 0.22 (see Table 3): when the smallest unit is
481 considered, almost 80% of the building peak load at design conditions is satisfied by the
482 back-up heater. The peak load ratio is related to the bivalent temperature of the system,
483 which is equal to -5°C, 0°C and +5°C when HP₁, HP₂ and HP₃ are respectively considered
484 for HHP systems, and is lower than the design temperature for the reference heating
485 system based on HP₀.

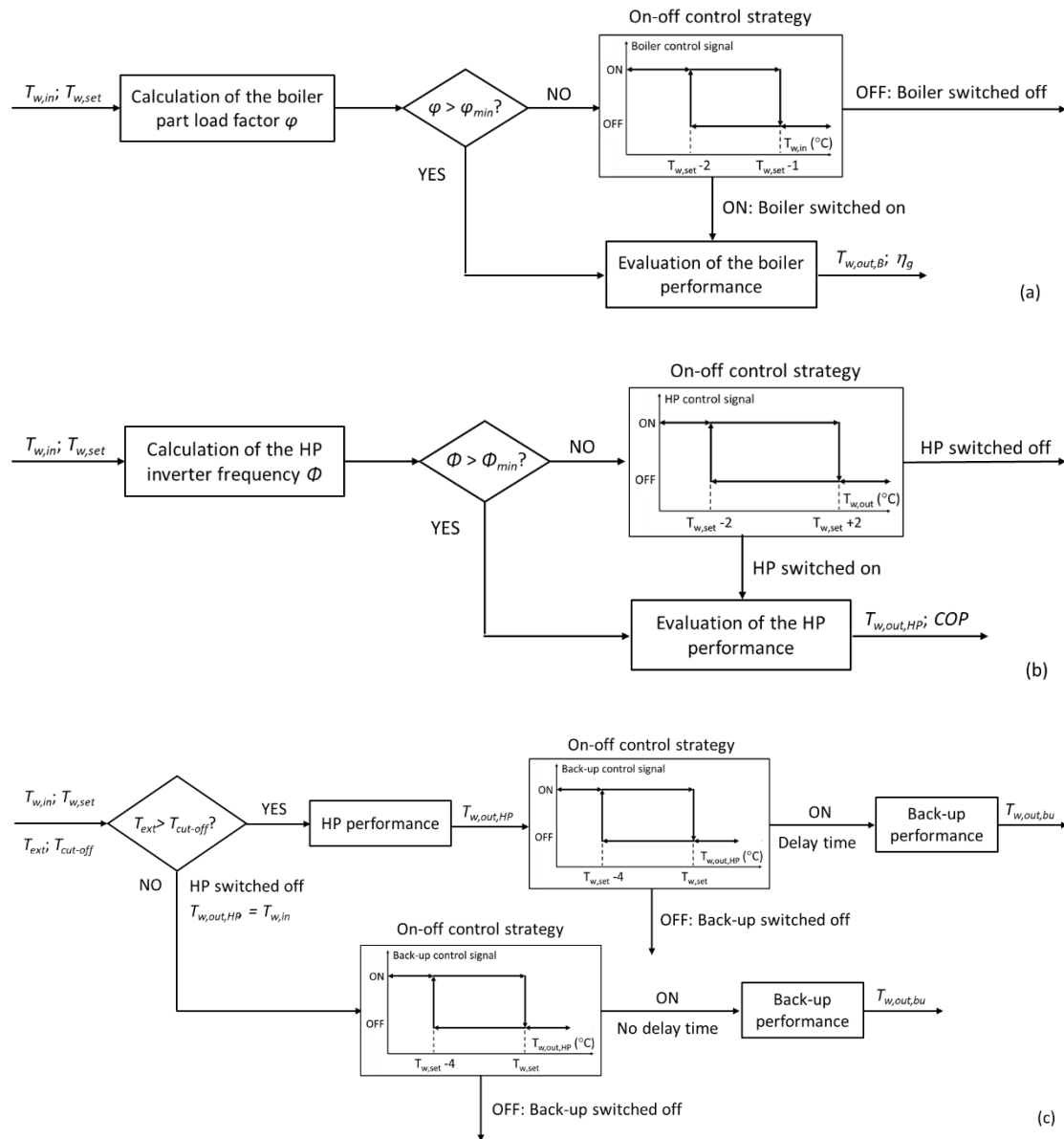
486

487 **2.4. Control strategies of the heating systems**

488 The gas boiler control logic is based on a PI controller coupled to an on-off algorithm.
489 The flow chart of the boiler control strategy is shown in Figure 6a, as a reference. As long
490 as the boiler load factor φ is between the declared modulating range reported in Table 1
491 (i.e. between 1 and 0.25), the boiler heating capacity is modulated to maintain the supply

492 water temperature equal to its set-point value, fixed by the climatic curve and depending
 493 on the current ambient temperature.

494



495 Figure 6. Control algorithm implemented in TRNSYS for the gas boiler (a), the AWHP (b) and the hybrid
 496 system configurations (c)

497

498 On the other hand, when the device delivers the minimum thermal power and no further
 499 modulation is possible, the unit performs a series of on-off cycles to balance the building

500 heat load. The monitored variable during this operating mode is the return water
501 temperature, $T_{w,in}$: the boiler is switched off when $T_{w,in}$ becomes higher than $T_{w,set} - 1$ K
502 and it is then switched on when $T_{w,in}$ is lower than $T_{w,set} - 2$ K. The dead-band is needed
503 to prevent frequent oscillations of the boiler control signal and to limit the unit cycling
504 frequency.

505 As illustrated in Figure 6b, the heat pump control strategy is similar to that of the boiler:
506 a PI controller is adopted to set the inverter frequency and an on-off logic is activated
507 during the milder part of the season when the minimum frequency is reached. The heat
508 pump control system uses the supply water temperature at the outlet of the unit ($T_{w,out,HP}$)
509 as monitored variable and compares it to the set-point value imposed by the climatic
510 curve. By means of the PI algorithm, the inverter frequency is set to adapt the heat pump
511 heating capacity to the building heat load. For each unit considered in this work, the PI
512 parameters have been fixed to the same values: proportional gain K_p and integral time t_i
513 have been set to 5 and 300 s, respectively. As pointed out by the technical data reported
514 in Table 2, the inverter modulation range broadens from 15 Hz to 115 Hz. When the
515 building energy demand is low and the minimum frequency is reached, the heat pump
516 operates as a fixed-speed unit and the on-off control logic is introduced. This on-off
517 algorithm is characterized by a hysteresis cycle of amplitude 4 K centered around the
518 supply water set-point temperature, $T_{w,set}$. The adopted dead-band allows to reduce the
519 oscillations of the heat pump control signal, lowering both energy losses and compressor
520 mechanical stress.

521 On the other hand, HHP systems (i.e. cases #2 - #7 in Table 3) are characterized by two
522 devices which have to be independently activated. The back-up heater control strategy

523 has to satisfy several constraints in order to avoid energy losses and guarantee thermal
524 comfort for building users:

- 525 1. for parallel operating mode (i.e. when $T_{cut-off} < T_{ext} < T_{biv}$) the back-up device is
526 switched on only when the heat pump is activated and its heating capacity is lower
527 than the building load;
- 528 2. the back-up device has to limit its on-off cycle frequency;
- 529 3. a fixed delay for the back-up generator activation must be introduced to avoid
530 unnecessary operations, for example after a heat pump defrost cycle.

531 In Figure 6c the detailed flow chart of the control algorithm implemented for HHP
532 systems is shown. The back-up device control logic uses the water temperature at the
533 outlet of the heat pump as monitored variable and is characterized by an on-off control
534 strategy based on a hysteresis cycle: the back-up heater is activated when $T_{w,out,HP}$ is 4 K
535 lower than the supply water set-point temperature ($T_{w,set}$) and is then switched off when
536 $T_{w,out,HP}$ returns higher than $T_{w,set}$.

537 As stated previously, the back-up heater is not directly activated when the water
538 temperature at the heat pump outlet starts to decrease: a delay time, t_{del} , equal to 15
539 minutes has been introduced before the activation of the back-up system. This value has
540 been set in order to obtain the best compromise between two opposite aspects: energy
541 consumptions of the system and indoor comfort conditions. In fact, with a short delay
542 time, the back-up heater would be switched on even if unnecessary, maintaining optimal
543 comfort conditions within thermal zones but with larger energy consumptions; on the
544 contrary, the increase of the delay time causes a worsening of indoor thermal comfort,
545 since the back-up device would be activated when the supply water temperature is far
546 below its set-point value.

547 Finally, when the pure alternative or the alternative-parallel operating mode are activated,
548 a further control logic has been implemented. For configurations #5 - #7 (see Table 3),
549 characterized by a gas boiler as back-up device, the cut-off temperature ($T_{cut-off}$) is
550 introduced: when the outdoor temperature is lower than $T_{cut-off}$, the heat pump is
551 completely disabled and no delay time is considered for the activation of the boiler. On
552 the contrary, when T_{ext} is between $T_{cut-off}$ and T_{biv} , both heat generators are activated: in
553 this case the back-up heater is activated with the delay time of 15 minutes previously
554 introduced.

555 In this study, different values of $T_{cut-off}$ have been considered in order to assess the
556 influence of the control strategy on the energy performance of HHP systems; for each
557 configuration, a series of simulations has been performed, defining five cut-off
558 temperatures ranging from the outdoor design temperature (i.e. -9°C) and an upper limit
559 fixed to 5°C .

560

561 **2.5. Key performance indicators**

562 In order to evaluate the seasonal efficiency of HHP systems in which different heaters
563 (i.e. boilers, heat pumps and electric resistances) are fed with different energy vectors (i.e.
564 electric energy (ee) and natural gas (gas)), and with the aim to compare the seasonal
565 energy performance of all the considered configurations, the system seasonal efficiency,
566 η_s , has been defined [in Eq. 2](#) as the ratio between the total amount of thermal energy
567 supplied by the heating system to the building, $E_{th,tot}$, and the total primary energy
568 consumption of the system, $E_{p,tot}$:

569

$$\eta_S = \frac{E_{th,tot}}{E_{p,tot}} = \frac{\sum_j E_{th,j}}{\sum_j \sum_i E_{p,i,j}} \text{ with } j=B, ER, HP \text{ and } i= ee, gas \quad (2)$$

570

571 where $E_{th,j}$ and $E_{p,i,j}$ are the thermal energy supplied to the building by the j-th heater along
 572 the season and the seasonal primary energy demand of the j-th heater linked to the i-th
 573 energy vector, respectively. Furthermore, $E_{p,i,j}$ is calculated starting from the seasonal
 574 energy consumption of the j-th heat generator linked to the i-th energy vector ($E_{i,j}$),
 575 multiplied for the corresponding primary energy conversion factor (PEF_i), as shown in
 576 the following Equation:

577

$$E_{p,i,j} = E_{i,j} PEF_i \text{ with } j=B, ER, HP \text{ and } i= ee, gas \quad (3)$$

578

579 The values of PEF_i fixed by Italian law [44] for electric energy and natural gas are equal
 580 to 2.42 and 1.05, respectively; these values have been used in the analysis presented in
 581 this work.

582 A series of additional performance indicators can be associated to the single heaters of
 583 HHP systems; for the heat pump, the condensing gas boiler and the electric heater, the
 584 $SCOP_{net}$, the seasonal boiler efficiency η_B and the electric heater efficiency η_{ER} are
 585 introduced in Eqs. 4, 5 and 6, respectively

586

$$SCOP_{net} = \frac{E_{th,HP}}{E_{HP,ee}} \quad (4)$$

$$\eta_B = \frac{E_{th,B}}{E_{B,gas}} \quad (5)$$

$$\eta_{ER} = \frac{E_{th,ER}}{E_{ER,ee}} \quad (6)$$

587

588 For the electric heater, a seasonal efficiency equal to 1 is assumed.

589 The methodology reported by the European standard EN 14825 [45] has been used to

590 evaluate the heat pump seasonal coefficient of performance, $SCOP_{net}$, for heating systems

591 based on a heat pump (i.e. configurations #1 - #7 of Table 3). Following EN 14825 for

592 HHP systems with a back-up based on an electric heater (i.e. configurations #2 - #4 in

593 Table 3), the heating seasonal coefficient of performance of the system, $SCOP$, is [here](#)

594 ~~introduced~~defined as:

595

$$SCOP = \frac{E_{th,HP} + E_{th,ER}}{E_{HP,ee} + E_{ER,ee}} \quad (7)$$

596

597 **3. RESULTS AND DISCUSSION**

598 In order to investigate the influence of back-up heater typology and heat pump size on

599 the seasonal energy efficiency of the whole system, a first series of simulations has been

600 performed selecting the cut-off temperature of HHP systems equal to the outdoor design

601 temperature for all cases. Therefore, for hybrid configurations, both heaters are activated

602 in parallel during the whole heating season with priority on the heat pump, considered as

603 the main heater of the system. Moreover, in these simulations both the defrost and cycling

604 losses have been considered.

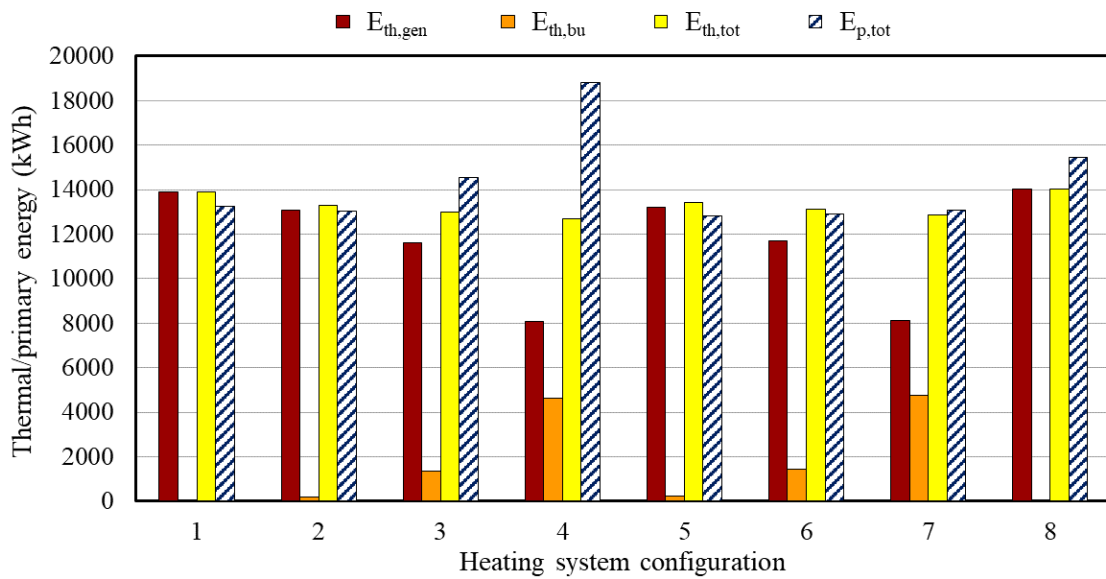
605 In Figure 7 the thermal energy supplied to the building by the whole heating system

606 ($E_{th,tot}$) and the total primary energy consumption ($E_{p,tot}$) are reported for the simulated

607 cases. Moreover, the thermal energy supplied to the building by both the back-up device

608 and the main heater (i.e. $E_{th, bu}$ and $E_{th, gen}$, respectively) is shown in the same figure as
 609 well. It is important to highlight that $E_{th, bu}$ is equal to $E_{th, ER}$ for cases #2 - #4 and to $E_{th, B}$
 610 for cases #5 - #7, while $E_{th, gen}$ corresponds to $E_{th, HP}$ for cases #1 - #7 and to $E_{th, B}$ for case
 611 #8. Obviously, $E_{th, gen}$ corresponds also to $E_{th, tot}$ for cases #1 and #8, since the heat pump
 612 and the boiler are the only heat generators in these configurations.

613



614

615 *Figure 7. Thermal energy delivered to the building by the main heater and by the back-up device and*
 616 *primary energy consumption of the system*

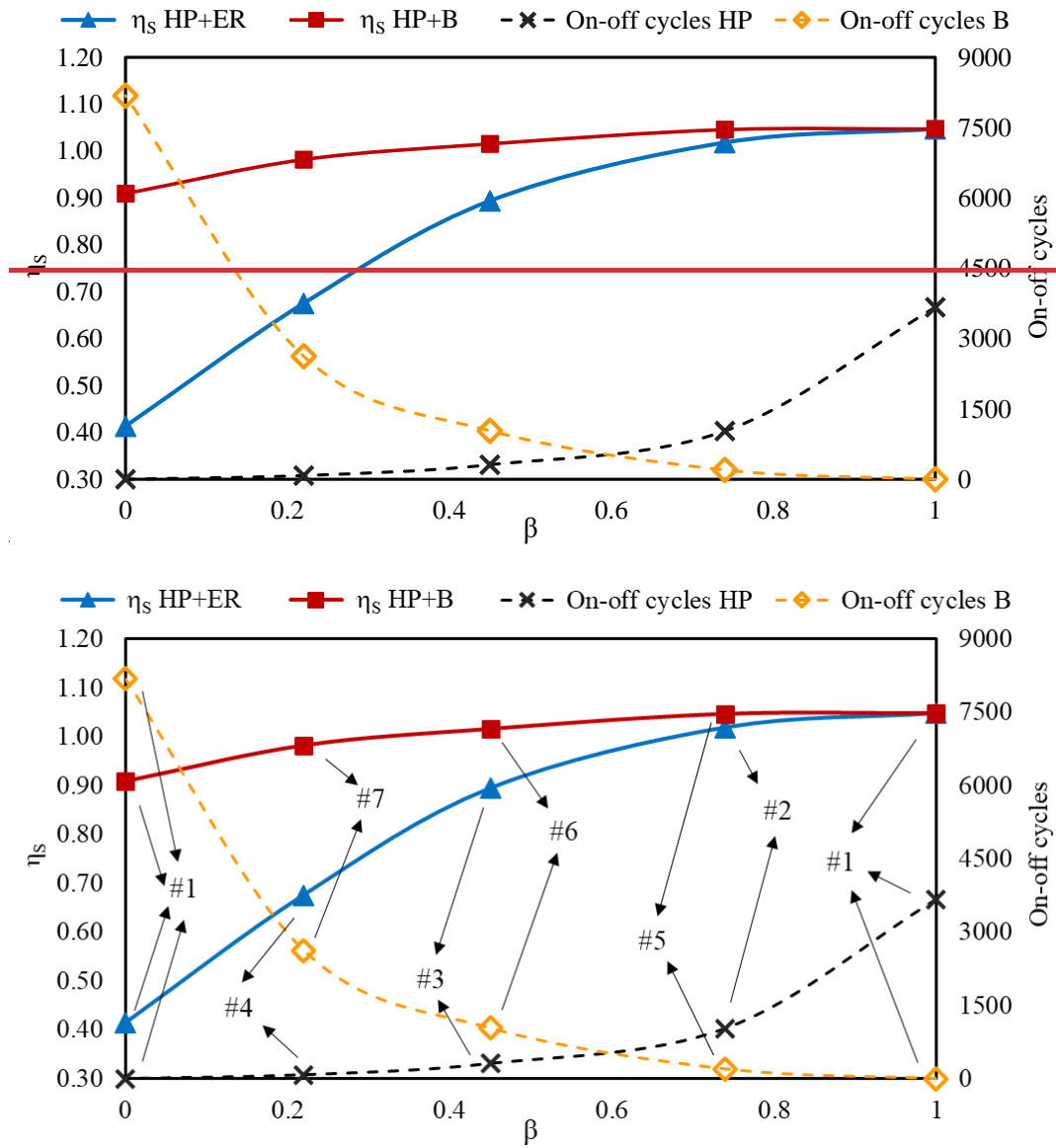
617

618 The reference system based on the single heat pump as heater (HP₀, case #1) is able to
 619 guarantee a lower primary energy consumption with respect to the condensing gas boiler
 620 (case #8). This quantity is slightly reduced when HHP systems are used in presence of
 621 both electric heaters (case #2) and gas boilers (case #5, #6 and #7) as back-up devices.
 622 These results confirm the conclusion made by Klein et al. [29], for which the maximum
 623 efficiency of HHP systems is achieved with heat pumps sized to cover only a fraction of
 624 the design load. If an electric heater is used as back-up, the heat pump has to be sized in
 625 order to cover at least 70% of the design heat load in order to minimize the total primary

626 energy consumptions. On the contrary, smaller heat pumps (down to 40% of the design
 627 thermal load) can be adopted if a boiler is used as back-up unit.

628

629



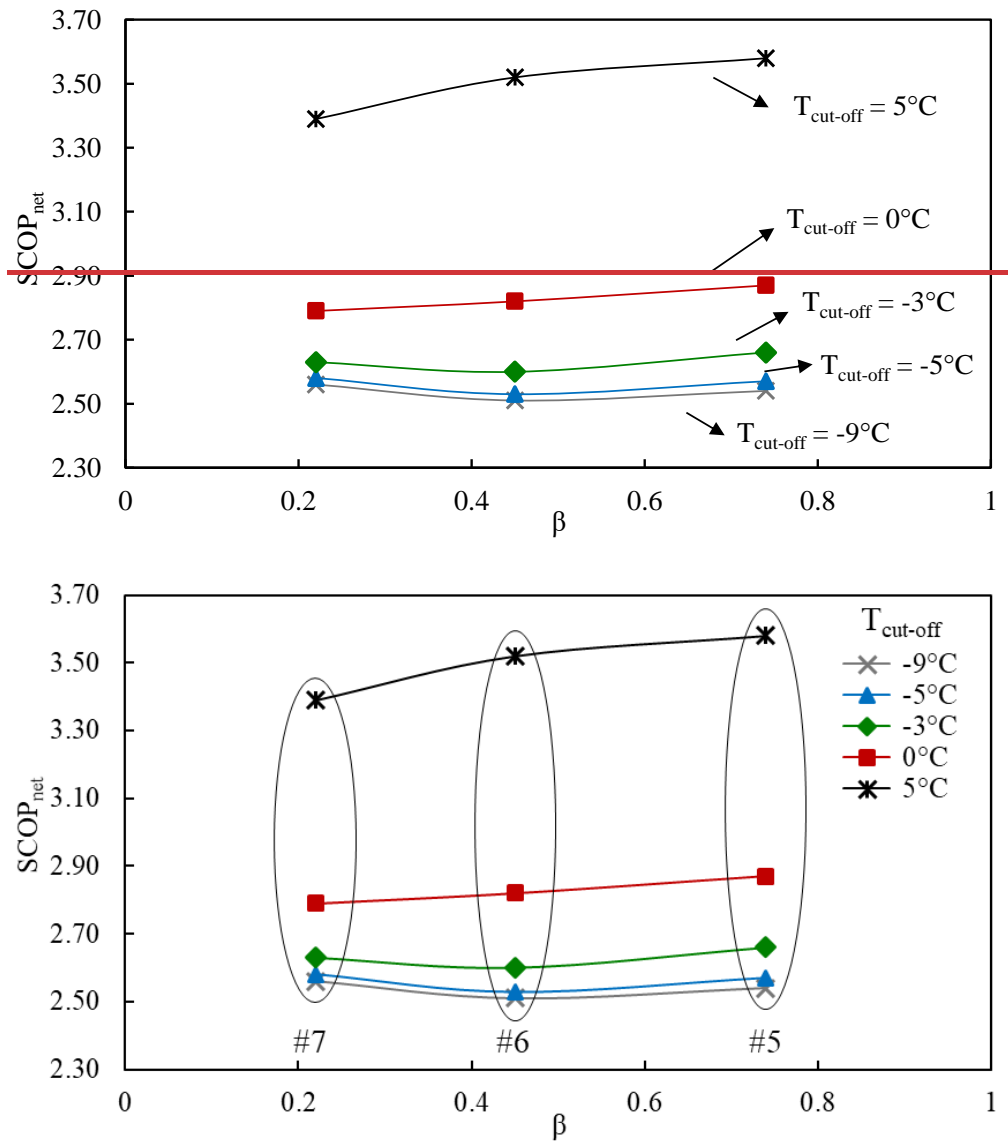
630

631 *Figure 8. Seasonal energy efficiency of the system, heat pump and boiler seasonal on-off cycles as*
 632 *functions of the building peak load ratio*
 633

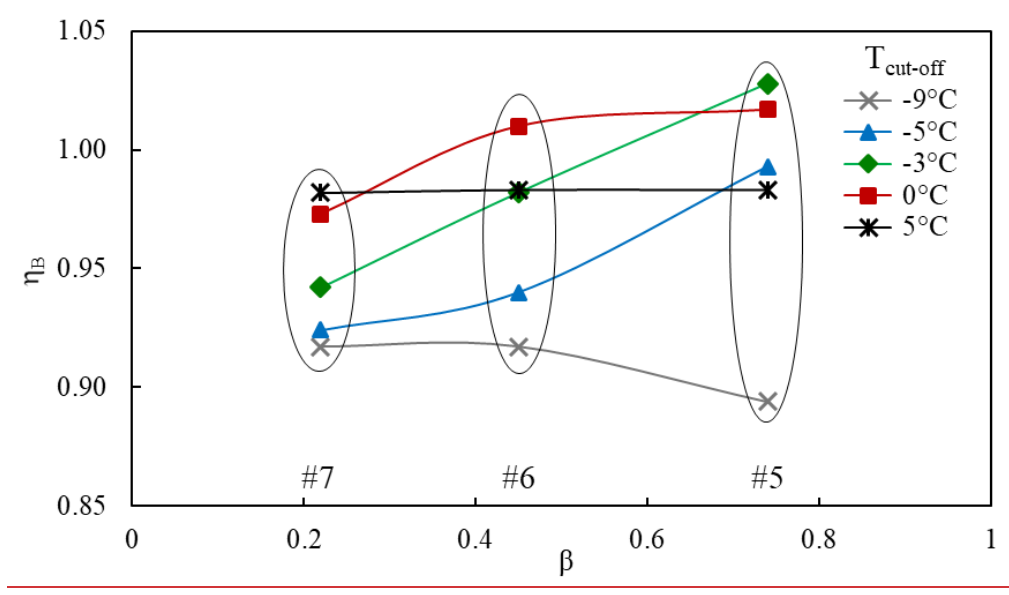
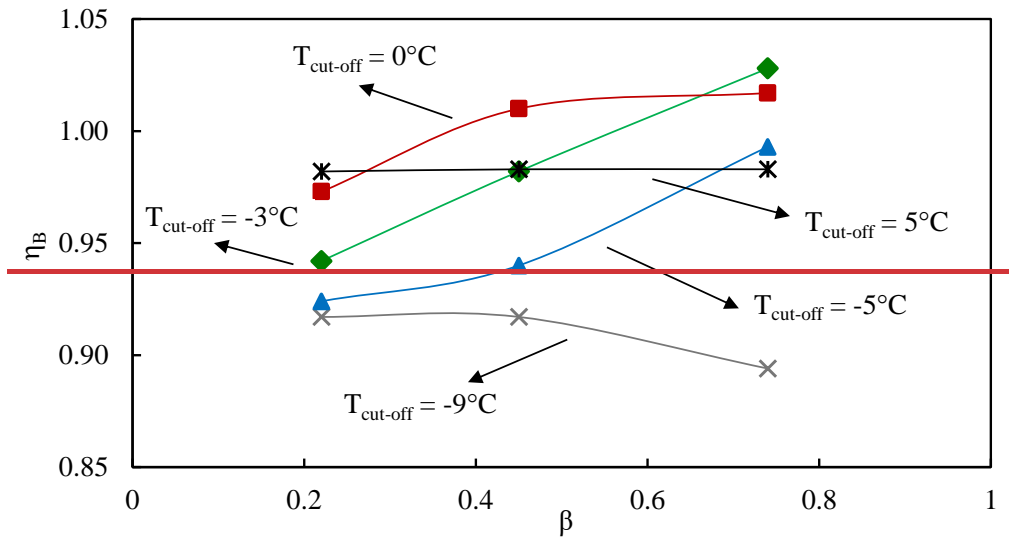
634 In Figure 8 the seasonal energy efficiency of the system, η_s , and the total number of on-
 635 off cycles carried out by the heat pump and the boiler are shown as functions of the
 636 building peak load ratio for all the simulated cases. It is evident from Figure 8 that when

637 the size of the heat pump is reduced with respect to the design heat load, the number of
638 on-off cycles performed by the heat pump is strongly reduced, decreasing from 3666
639 cycles for case #1 to 80 cycles for cases #4 and #7 (-98%). Indeed, with undersized heat
640 pumps, on-off cycling must be used to adapt the unit heating capacity to the building heat
641 load only in the milder part of the heating season. The number of on-off cycles carried
642 out by the heat pump is independent from the typology of back-up unit: as a consequence,
643 when undersized devices are used in HHP systems, the energy losses linked to on-off
644 cycles are reduced and, for this reason, the energy performance of the heat pump is
645 improved. Nevertheless, the considered heat pumps are equipped with an EEV: since with
646 this kind of expansion valves the energy penalization linked to each on-off cycle is low,
647 the enhancement of the heat pump seasonal performance is significant only for units
648 characterized by a peak load ratio lower than 0.5. On the contrary, the number of defrost
649 cycles performed by the heat pump does not change since the control strategy for the
650 activation of the defrosting transient depends on the outdoor conditions and the
651 parameters of its algorithm are the same for each case. Results point out that, in fact, the
652 heat pumps used as main generator in cases #1 - #7 carry out the same number of defrost
653 cycles along the heating season (1491) and, for this reason, the impact of defrosting
654 energy losses on η_s has the same order of magnitude for all pure parallel configurations.
655 As it will be reported in detail in a following section of the paper, the seasonal efficiency
656 of the system has a penalty larger than 7% due to defrost cycles.

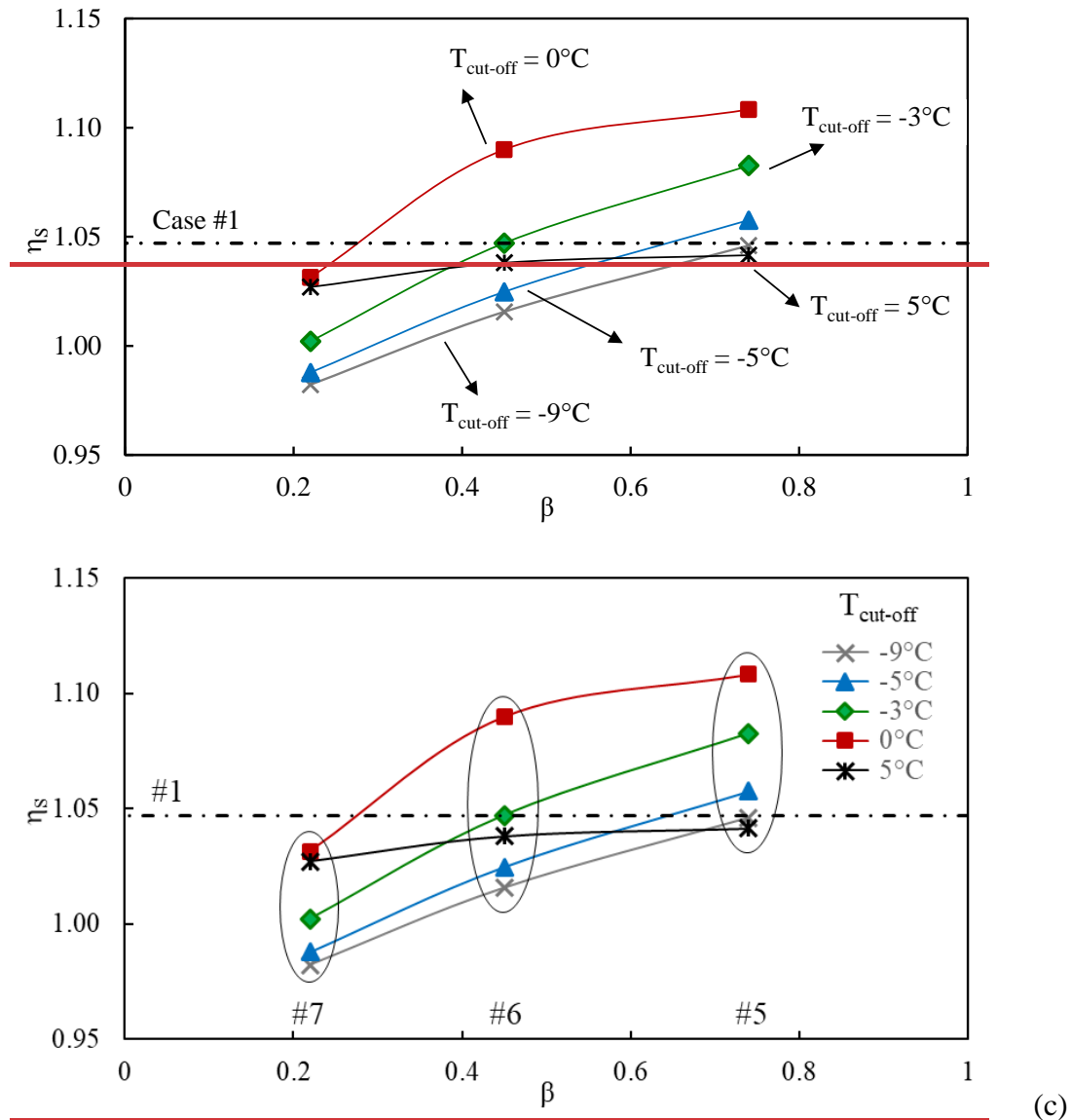
657 Furthermore, in order to satisfy the building required load, the smaller heat pumps are
658 called to operate at larger inverter frequency with respect to the heat pumps sized on the
659 building peak load (case #1) and, as pointed out by Figure 3, their seasonal *COP* values
660 are lower.



(a)



(b)



662 Figure 9. Seasonal energy performance indicators of the studied systems as functions of the peak load
 663 ratio and of the cut-off temperature: $SCOP_{\text{net}}$ (a), η_B (b) and η_s (c)
 664

665 A second series of simulations was focused on the role played by the choice of the cut-
 666 off temperature on the seasonal energy performance of HHP systems fed by two energy
 667 vectors (i.e. case #5, #6 and #7, with a gas boiler as back-up heater). The seasonal
 668 efficiency of the system has been calculated for different values of the cut-off temperature
 669 and compared to that obtained for case #1 (i.e. a monovalent system based on the heat
 670 pump HP_0): Figure 9 highlights the influence of $T_{\text{cut-off}}$ and of the peak load ratio, β , on

671 the seasonal energy performance indicators of the system (i.e. $SCOP_{net}$, η_B and η_S , see
672 [Eqs. 4, 5 and 2, respectively](#)).

673 Figure 9 shows that significant primary energy savings can be obtained by adopting an
674 alternative hybrid system configuration if compared to conventional monovalent heating
675 systems based on an AWHP or a condensing gas boiler. Moreover, there exists for each
676 specific application an optimal configuration of the HHP system for which η_S assumes its
677 maximum value. In our case study, the largest value of η_S is obtained for $\beta=0.74$ (case
678 #5), setting the cut-off temperature equal to 0°C . Under these conditions, the seasonal
679 efficiency of the heating system can be enhanced up to +6% and +22% with respect to
680 the reference cases #1 and #8, in which a single heat generator is used (i.e. an AWHP and
681 a condensing gas boiler, respectively). Moreover, it is evident from Figure 9c that a
682 similar trend of η_S as a function of the cut-off temperature is obtained for all the values
683 of the peak load ratio. Indeed, in the present study, for each value of the bivalent
684 temperature, η_S increases when $T_{cut-off}$ increases and presents a maximum in
685 correspondence of 0°C . However, the optimal value of the cut-off temperature depends
686 on the climatic conditions of the site and in presence of mild winter conditions (in terms
687 of both outdoor air temperature and humidity) can shift towards the design temperature,
688 which means heat pump active for a longer time.

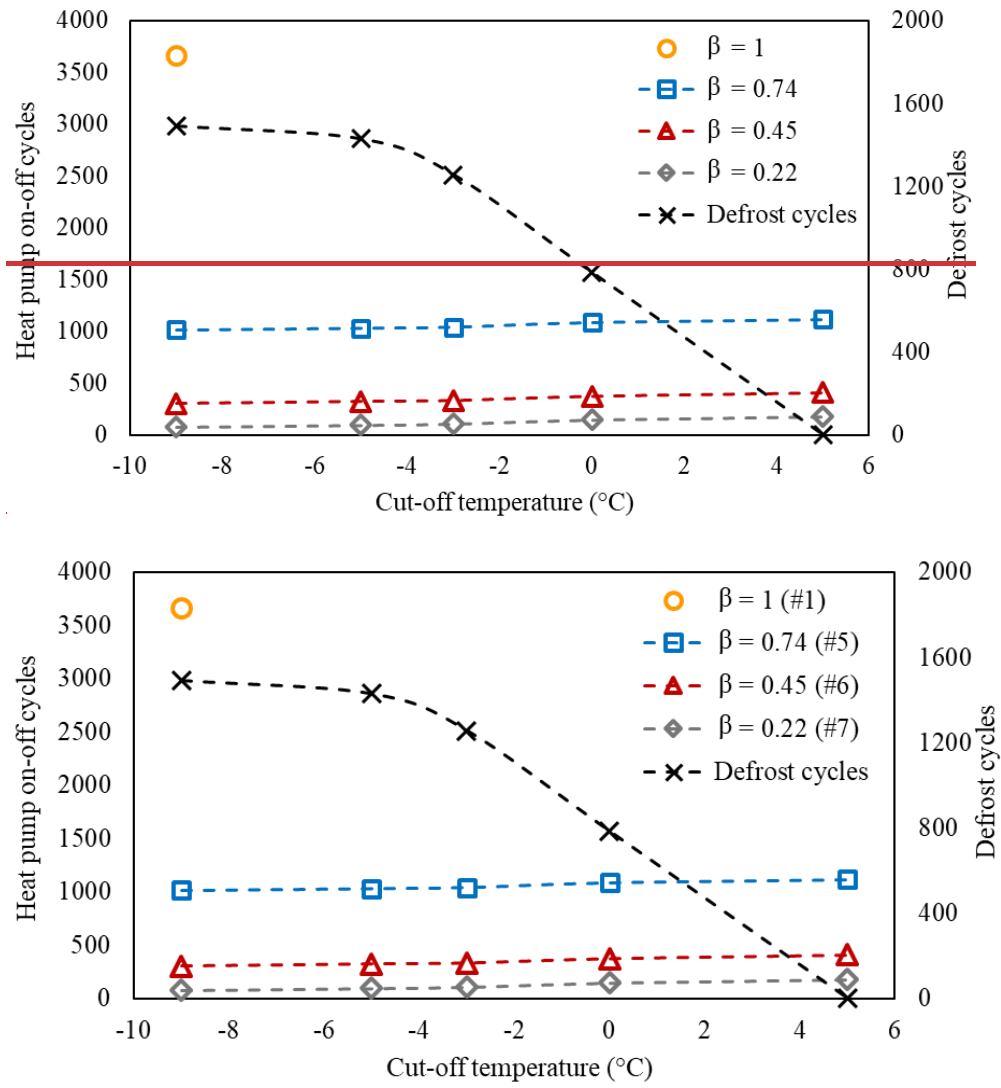
689 The energy performance results can be fully explained by observing Figure 9a and Figure
690 9b, in which the values of $SCOP_{net}$ and η_B are respectively shown as functions of the peak
691 load ratio and of the cut-off temperature. First, it is evident that for each heat pump size
692 (i.e. for all values of β) the seasonal energy performance of the unit monotonically
693 increases when the cut-off temperature increases. In fact, when the heat pump size is
694 reduced, its $SCOP_{net}$ is improved for two reasons: i) when $T_{cut-off}$ increases, the number of

695 defrost cycles performed by the heat pump decreases, as will be highlighted in a following
696 figure; ii) the period in correspondence of which the heat pump operates with low *COP*
697 values, due to low external temperatures and large compressor frequency, is strongly
698 reduced.

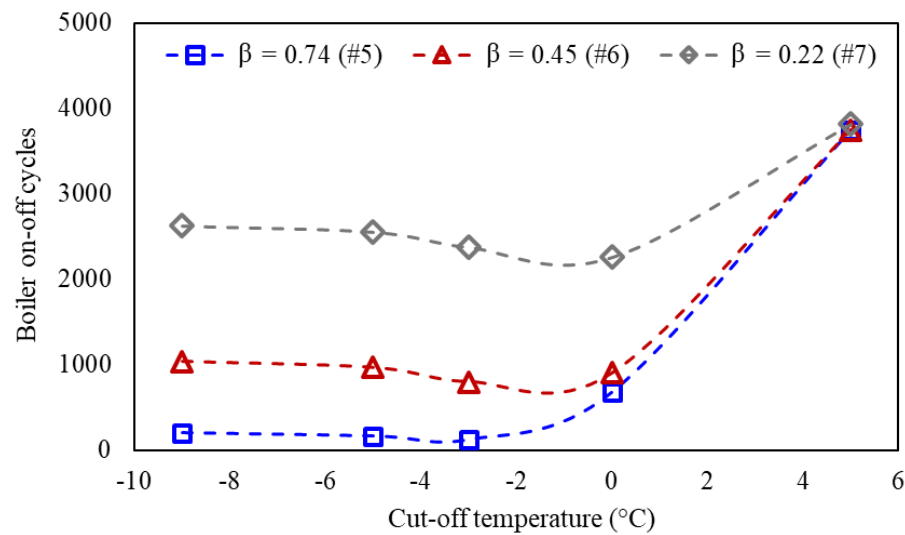
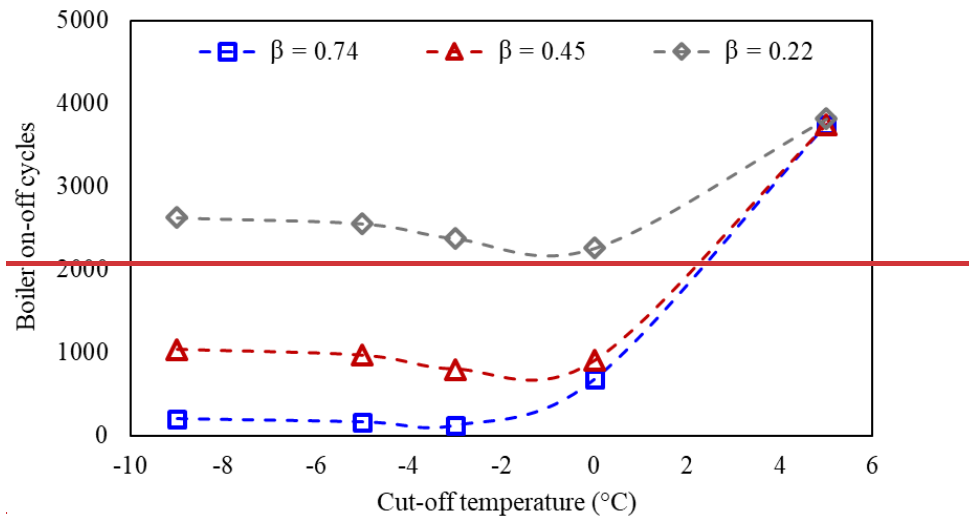
699 It is important to stress that when the peak load ratio is decreased, an increasing share of
700 the building heat demand is supplied by the back-up boiler and, for this reason, the energy
701 performance of the whole HHP system is more influenced by the boiler seasonal
702 efficiency. As reported by Figure 9b, η_B is characterized by different trends when the
703 peak load ratio decreases: for each configuration, the boiler seasonal efficiency has its
704 maximum value in correspondence of a cut-off temperature close to the corresponding
705 bivalent temperature (-3°C , 0°C and 5°C for cases #5, #6 and #7, respectively). In all
706 cases, η_B is characterized by a monotonic increasing trend when $T_{cut-off}$ is lower than T_{biv} :
707 when the cut-off temperature increases, the HHP system operates for a longer time in
708 alternative mode (i.e. with the back-up as the unique active heat generator) and the boiler
709 performance becomes more and more influent on the system overall efficiency.

710 In Figure 10a the annual number of defrost and on-off cycles performed by the air-to-
711 water heat pumps are reported as functions of the cut-off temperature and of the peak load
712 ratio. It is evident that the higher the cut-off temperature, the lower the number of defrost
713 cycles carried out by the heat pump. For example, when $T_{cut-off}$ is set equal to 0°C , the
714 number of defrost cycles is reduced up to 47% with respect to pure parallel configurations
715 (i.e. $T_{cut-off}$ equal to T_{des}), while defrosting energy losses can be completely avoided in the
716 site considered in these simulations for $T_{cut-off}$ equal to 5°C .

717



(a)



(b)

718 Figure 10. Seasonal number of defrost cycles, heat pump on-off cycles (a) and boiler on-off cycles (b) as
 719 functions of the peak load ratio and of the cut-off temperature
 720

721 Moreover, the data depicted in Figure 10a highlight that the cut-off temperature has no
 722 significant influence on the cycling frequency of the heat pump: for a fixed value of the
 723 peak load ratio the number of on-off cycles performed by the heat pump during the
 724 heating season slightly raises when $T_{cut-off}$ increases. Furthermore, if compared to case #1
 725 the number of on-off cycles diminishes up to 70%, 90% and 95% when the peak load
 726 ratio goes from 1 to 0.74, 0.45 and 0.22, respectively. However, this large reduction of

727 performed cycles is not able to guarantee noticeable enhancement of the heat pump
728 seasonal performance due to the low cycling energy losses of the selected units.
729 On the other hand, also the boiler seasonal efficiency is influenced by the number of on-
730 off cycles carried out along the season, depicted in Figure 10b as a function of both the
731 peak load ratio and the cut-off temperature. It is evident that the number of on-off cycles
732 performed by the boiler raises when $T_{cut-off}$ increases and the heat pump size is reduced,
733 according to a more frequent use of the back-up unit in place of the AWHP. For example,
734 by fixing the cut-off temperature equal to -5°C , the number of cycles carried out by the
735 boiler increases from 160 to 2551 when the peak load ratio decreases from 0.74 to 0.22;
736 as a consequence, the boiler seasonal efficiency is reduced up to 7%.

737

738 Table 4. Influence of on-off cycles and defrost cycles on the seasonal energy efficiency
739 of the system for cases #1 and #8

| | Case #1 | | | | | Case #8 | |
|----------|---------------------------------|------------------------|------------------------|------------------------------------|---------------------|------------------------|--|
| | With defrost and cycling losses | Without defrost losses | Without cycling losses | Without defrost and cycling losses | With cycling losses | Without cycling losses | |
| η_s | 1.05 | 1.13 | 1.06 | 1.14 | 0.91 | 1.01 | |
| Δ | - | +7.6% | +0.9% | +8.6% | - | +11% | |

740

741 In order to put in evidence the influence of the energy losses of both defrost and on-off
742 cycles on the performance of the system, the seasonal energy performance (η_s) of

743 monovalent configurations (i.e. case #1 and case #8) has been evaluated neglecting the
744 penalization effect linked to on-off and defrost cycles. In
745 Table 4 the system seasonal energy efficiency is reported for different conditions, by
746 considering or neglecting the effect of on-off and defrost cycles for cases #1 and #8.
747 The influence of the cycling losses on the seasonal performance factor of the heat pump
748 (i.e. case #1) is negligible: according to the data shown in
749 Table 4, the seasonal efficiency η_s decreases less than 1% due to on-off cycles. This result
750 was expected since, as reported before, the considered heat pump is equipped with an
751 EEV, which guarantees reduced penalization during on-off transients. On the contrary,
752 defrost cycles energy losses have a significant impact on the heat pump seasonal
753 efficiency: η_s varies from 1.13 of the ideal case, in which defrost cycles have not been
754 considered, to 1.05, corresponding to a reduction larger than 7% on a seasonal basis. Of
755 course, this result depends on the chosen location, which is characterized by a cold and
756 humid winter in this case study, but this result highlights how the energy losses linked to
757 defrosting cycles can be considered significant in ambient conditions typical of large part
758 of Northern Italy, with an expected penalty on η_s ranging around 5-15%. This result
759 underlines how, in order to evaluate in an accurate way the energy and economic
760 feasibility of these hybrid systems, the energy losses linked to the defrosting cycles has
761 to be always taken into account. Finally, it is evident that cycling losses play a significant
762 role on the boiler seasonal performance: as reported in
763 Table 4 for case #8, its seasonal efficiency decreases up to 10% due to on-off cycle energy
764 penalties. In fact, as evidenced by Figure 8, during the winter season the boiler performs
765 a higher number of cycles with respect to the heat pump (more than 8000 cycles along
766 the season) and, additionally, it is characterized by larger energy losses for each cycle

767 (see Table 1). For these reasons, on-off cycling losses cannot be neglected in dynamic
768 simulations for hybrid systems in which a boiler is present.

769 In conclusion, HHP systems are able to guarantee slight primary energy savings if
770 compared to conventional heating systems based on a single AWHP as heat generator (up
771 to 6%), while a stronger reduction of the system primary energy consumption, up to 22%,
772 can be obtained by hybrid configurations with respect to monovalent heating systems
773 based on a gas boiler. The results of the simulations presented in this work highlight how
774 the energy performance of this kind of systems can be improved if the heat pump size
775 (thus, the peak load ratio) is optimized on the basis of the adopted back-up heater and, at
776 the same time, if an optimal setting of the system control algorithm is done.

777

778 **4. CONCLUSIONS**

779 In this paper a numerical study on the energy performance during the heating season of
780 hybrid heat pump (HHP) systems coupled to a reference residential building has been
781 performed by means of a series of dynamic simulations made with TRNSYS. The hybrid
782 systems investigated in this work are based on an air-to-water heat pump (AWHP), while
783 an electric heater or a condensing gas boiler have been considered as back-up devices.
784 These systems have been compared to traditional monovalent configurations (heat pump
785 only or gas-fired boiler only) in order to assess the optimal ~~system~~ layout of the heating
786 system which can guarantee the maximum primary energy savings.

787

788 ~~The results presented in this paper confirm~~ Hence, based on the obtained results, it is clear

789 how the use of HHP systems could ensure significant primary energy savings if compared
790 to conventional monovalent systems based on a single heat generator and these benefits

791 strongly depend on the heat pump size, the back-up heater typology and the control
792 strategy adopted for the activation of both the devices. The following statements
793 concerning hybrid heat pump systems can be made:

794 • ~~w~~When the cut-off temperature is set equal to the design temperature (i.e. pure
795 parallel working mode), only a slight improvement of the system seasonal
796 efficiency can be achieved with respect to traditional configurations, although a
797 strong reduction of the heat pump on-off cycles is observed. In this case, the heat
798 pump must be sized to satisfy at least 40% and 70% of the building design load,
799 when a boiler or an electric heater are selected as back-up devices, respectively.

800 • ~~On the other hand,~~ when a gas-fired boiler is considered as back-up heater and
801 for the alternative operating mode (i.e. when $T_{cut-off}$ is larger than T_{ext}), it is possible
802 to define an optimal configuration of the system which maximizes its seasonal
803 energy performance. For the site considered in these simulations and for each size
804 of the heat pump, the maximum value of η_s is obtained when $T_{cut-off}$ is set equal to
805 0°C .

806 • ~~and~~ appreciable primary energy savings (up to 6% and to 22% with respect to the
807 reference monovalent configurations based on an AWHP and a condensing gas
808 boiler, respectively) can be achieved with a peak load ratio equal to 0.74 (which
809 means that the heat pump is sized in order to cover up to 74% of the design thermal
810 load).

811 • ~~Finally, results point out that~~ defrost cycles have a significant influence on the
812 system seasonal energy efficiency (η_s), which is decreased between 5% and 15%
813 in cold and humid climates, typical of Northern Italy, as the one considered in this
814 paper.

- 815 • ~~On the other hand~~, the effect of cycling losses is strictly correlated to the features
816 of each heater: the results shown in this paper demonstrate how on-off cycles do
817 not significantly affect the heat pump performance in presence of an EEV and a
818 large inverter modulating range, while, on the contrary, cycling losses have a
819 significant impact on the boiler seasonal efficiency especially for units with a
820 limited modulating range.

821

822 REFERENCES

- 823 [1] R.A. Enker, G.M. Morrison, Analysis of the transition effects of building codes and
824 regulations on the emergence of a low carbon residential building sector, Energy and
825 Buildings 156 (2017) 40-50.
- 826 [2] European Union, Directive 2010/31/EU of the European Parliament and of the
827 Council of 19 May 2010 on the Energy Performance of Buildings, European Union,
828 Brussels, Belgium, 2010.
- 829 [3] European Union, Directive 2012/27/EU of the European Parliament and of the
830 Council of 25 October 2012 on Energy Efficiency, amending Directives
831 2009/125/EC, European Union, Brussels, Belgium, 2012.
- 832 [4] European Union, Directive 2018/844 of the European Parliament and of the Council
833 of 30 May 2018 amending Directive 2010/31/EU on the Energy Performance of
834 Buildings and Directive 2012/27/EU on Energy Efficiency, Brussels, Belgium, 2018.
- 835 [5] European Commission, Communication from the Commission to the European
836 Parliament, the Council, the European economic and social Committee and the
837 Committee of the Regions – A policy framework for climate and energy in the period
838 from 2020 to 2030, European Commission, Brussels, Belgium, 2014.

- 839 [6] ISTAT (Italian National Statistical Institute), Census 2011 of population and houses,
840 2011. Available from [http://www.istat.it/it/censimento-popolazione/censimento-
842 popolazione-2011](http://www.istat.it/it/censimento-popolazione/censimento-
841 popolazione-2011).
- 842 [7] C. Treichel, C.A. Cruickshank, Greenhouse gas emissions analysis of heat pump
843 water heaters coupled with air-based solar thermal collectors in Canada and the
844 United States, *Energy and Buildings* 231 (2021) 110594.
- 845 [8] F. Knobloch, S.V. Hanssen, A. Lam, H. Pollitt, P. Salas, U. Chewpreecha, M.A.J.
846 Huijbregts, J.F. Mercure, Net emission reductions from electric cars and heat pumps
847 in 59 world regions over time, *Nature Sustainability* 3 (2020) 437-447.
- 848 [9] F. Madonna, F. Bazzocchi, Annual performances of reversible air-to-water heat
849 pumps in small residential buildings, *Energy and Buildings* 65 (2013) 299-309.
- 850 [10] EHPA (European Heat Pump Association), European Heat Pump Market and
851 Statistics Report 2015, 2016. Available from: [http://www.ehpa.org/market-
853 data/2015/](http://www.ehpa.org/market-
852 data/2015/).
- 853 [11] H. Wolisz, T. Schutz, T. Blanke, M. Hagenkamp, M. Kohn, M. Wesseling, D.
854 Muller, Cost optimal sizing of smart buildings' energy system components
855 considering changing end-consumer electricity markets, *Energy* 137 (2017) 715-728.
- 856 [12] M. Qu, T. Li, S. Deng, Y. Fan, Z. Li, Improving defrosting performance of cascade
857 air source heat pump using thermal energy storage based reverse cycle defrosting
858 method, *Applied Thermal Engineering* 121 (2017) 728-736.
- 859 [13] J.Y. Jang, H.H. Bae, S.J. Lee, M.Y. Ha, Continuous heating of an air-source heat pump
860 during defrosting and improvement of energy efficiency, *Applied Energy* 110 (2013)
861 9-16.

- 862 [14] Q. Minglu, X. Liang, S. Deng, J. Yiqiang, Improved indoor thermal comfort during
863 defrost with a novel reverse-cycle defrosting method for air source heat pumps,
864 Building and Environment 45 (2010) 2354-2361.
- 865 [15] G. Bagarella, R. Lazzarin, B. Lamanna, Cycling losses in refrigeration equipment:
866 An experimental evaluation, International Journal of Refrigeration 36 (2013) 2111-
867 2118.
- 868 [16] M. Pieve, R. Trinchieri, heat pump market report for Italy, Heat Pumping
869 Technologies Magazine 36 (2018) 14-18.
- 870 [17] L. Bergmann, J. Jansen, The State of Play of the Hybrid Heat Pump Market, Delta
871 Energy & Environment, 2015.
- 872 [18] H. Park, K.H. Nam, G.H. Jang, M.S. Kim, Performance investigation of heat pump-
873 gas fired water heater hybrid system and its economic feasibility study, Energy and
874 Buildings 80 (2014) 480-489.
- 875 [19] R. De Coninck, L. Helsen, Practical implementation and evaluation of model
876 predictive control for an office building in Brussels, Energy and Buildings 111 (2016)
877 290-298.
- 878 [20] G. Li, Parallel loop configuration for hybrid heat pump – gas fired water heater
879 system with smart control strategy, Applied Thermal Engineering 138 (2018) 807-
880 818.
- 881 [21] G. Li, Y. Du, Performance investigation and economic benefits of new control-
882 strategies for heat pump-gas fired water heater hybrid system, Applied Energy 232
883 (2018) 101-118.

- 884 [22] E. Zanetti, M. Aprile, D. Kum, R. Scoccia, M. Motta, Energy saving potentials of a
885 photovoltaic assisted heat pump for hybrid building heating system via optimal
886 control, *Journal of Building Engineering* 27 (2020) 100854.
- 887 [23] P. Fitzpatrick, F. D’Ettorre, M. De Rosa, M. Yadack, U. Eicker, D. P. Finn, Influence
888 of electricity prices on energy flexibility of integrated hybrid heat pump and thermal
889 storage systems in a residential building, *Energy & Buildings* 223 (2020) 110142.
- 890 [24] F. D’Ettorre, P. Conti, E. Schito, D. Testi, Model predictive control of a hybrid heat
891 pump system and impact of the prediction horizon on cost-saving potential and
892 optimal storage capacity, *Applied Thermal Engineering* 148 (2019) 524-535.
- 893 [25] T. S. Amirkhizi, I. G. Jensen. Cost comparison and optimization of gas electric hybrid
894 heat pumps. *WIRES Energy and Environment* (2020) e370.
- 895 [26] Y. Ma, M. Zaheeruddin, Dynamic modeling, adaptive control and energy
896 performance simulation of a hybrid hydronic space heating system, *Building Services
897 Engineering Research and Technology* 39 (2018) 406-429.
- 898 [27] G. Bagarella, R. Lazzarin, M. Noro, Annual simulation, energy and economic
899 analysis of hybrid heat pump systems for residential buildings, *Applied Thermal
900 Engineering* 99 (2016) 485-494.
- 901 [28] D. Fischer, K.B. Lindberg, H. Madani, C. Wittwer, Impact of PV and variable prices
902 on optimal system sizing for heat pumps and thermal storage, *Energy and Buildings*
903 128 (2016) 723-733.
- 904 [29] K. Klein, K. Huchtemann, D. Müller, Numerical study on hybrid heat pump systems
905 in existing buildings, *Energy and Buildings* 69 (2014) 193-201.
- 906 [30] C. Di Perna, G. Magri, G. Giuliani, G. Serenelli, Experimental assessment and
907 dynamic analysis of a hybrid generator composed of an air source heat pump coupled

908 with a condensing gas boiler in a residential building, *Applied Thermal Engineering*
909 76 (2015) 86-97.

910 [31] S.A. Klein et al., *TRNSYS 17: A Transient System Simulation Program*, Solar
911 Energy Laboratory, University of Wisconsin, Madison, WI, USA, 2010.

912 [32] D.A. Waddicor, E. Fuentes, M. Azar, J. Salom, Partial load efficiency degradation of
913 a water-to-water heat pump under fixed set-point control, *Applied Thermal*
914 *Engineering* 106 (2016) 275-285.

915 [33] M. Dongellini, G.L. Morini, On-off cycling losses of reversible air-to-water heat
916 pump systems as a function of the unit power modulation capacity, *Energy*
917 *Conversion and Management* 196 (2019) 966-978.

918 [34] R. Dott, M. Haller, J. Ruschenburg, F. Ochs, J. Bony, IEA-SHC Task 44 Subtask C
919 Technical Report: The Reference Framework for System Simulations of the IEA SHC
920 Task 44 / HPP Annex 38: Part B: Buildings and Space Heat Load, IEA-SHC, 2013.
921 (27th of October 2017).

922 [35] G. Bagarella, R. Lazzarin, M. Noro, Sizing strategy of on-off and modulating heat
923 pump systems based on annual energy analysis, *International Journal of Refrigeration*
924 65 (2016) 183-193.

925 [36] Q. Minglu, X. Liang, D. Shiming, J. Yiqiang, A study of the reverse cycle defrosting
926 performance on a multi-circuit outdoor coil unit in an air source heat pump – Part I:
927 Experiments, *Applied Energy* 91 (2012) 122-129.

928 [37] P. Vocale, G.L. Morini, M. Spiga, Influence of outdoor air conditions on the air
929 source heat pumps performance, *Energy Procedia* 45 (2014) 653-662.

- 930 [38] D. Huang, X. Yuan, X. Zhang, Effects of fan-starting methods on the reverse-cycle
931 defrost performance of an air-to-water heat pump, *International Journal of*
932 *Refrigeration* 27 (2004) 869-875.
- 933 [39] D. Huang, Q. Li, X. Yuan, Comparison between hot-gas bypass defrosting and
934 reverse-cycle defrosting methods on an air-to-water heat pump, *Applied Energy* 86
935 (2009) 1697-1703.
- 936 [40] A.T. De La Cruz, P. Riviere, D. Marchio, O. Cauret, A. Milu, Hardware in the loop
937 test bench using Modelica: A platform to test and improve the control of heating
938 systems, *Applied Energy* 188 (2017) 107-120.
- 939 [41] Italian Republic, DPR 412/93, Regolamento recante norme per la progettazione,
940 l'installazione, l'esercizio e la manutenzione degli impianti termici degli edifici ai
941 fini del contenimento dei consumi di energia, 1993.
- 942 [42] TRNSYS 17 - A TRaNsient SYstem Simulation program, User Manual. Volume 5:
943 Multizone Building Modeling with Type 56 and TRNBuild. Version 17.1,
944 Solar Energy Laboratory, University of Wisconsin, Madison, USA, 2012.
- 945 [43] M.F. Fels, PRISM: An introduction, *Energy and Buildings* 9 (1986) 5-18.
- 946 [44] Decreto interministeriale 26 giugno 2015 - Applicazione delle metodologie di calcolo
947 delle prestazioni energetiche e definizione delle prescrizioni e dei requisiti minimi
948 degli edifici, 2015.
- 949 [45] CEN (European Committee for Standardization), Standard EN 14825:2016. Air
950 Conditioners, Liquid Chilling Packages and Heat Pumps, with Electrically Driven
951 Compressors, for Space Heating and Cooling – Testing and Rating at Part Load
952 Conditions and Calculation of Seasonal Performance, 2016.